

Gas in Galaxies

Adam K. Leroy^a and Alberto D. Bolatto^b

^aDepartment of Astronomy, The Ohio State University, 140 West 18th Avenue, Columbus, OH 43210, USA

^bDepartment of Astronomy and Joint Space-Science Institute, University of Maryland, 4296 Stadium Drive, College Park, MD 20742, USA

© 20xx Elsevier Ltd. All rights reserved.

Chapter Article tagline: update of previous edition, reprint..

Glossary

Atomic gas interstellar material composed mostly of hydrogen in its neutral atomic state.

Molecular gas interstellar material composed mostly of hydrogen in its molecular state.

Ionized gas interstellar material composed mostly of hydrogen in its ionized state.

Main sequence of star-forming galaxies well-defined relationship between star formation rate and stellar mass found for star-forming disk galaxies.

Nomenclature

ISM	Interstellar medium
H _I	Atomic hydrogen
H ₂	Molecular hydrogen
H _{II}	Ionized hydrogen
GMC	Giant molecular cloud
kpc	kiloparsec

Abstract

In this chapter, we give an overview of the major components of the interstellar medium (ISM) in galaxies at a level appropriate for upper level undergraduates or beginning graduate students. We discuss the major constituents of the the ISM in present-day star forming galaxies and summarize common methods to observe these components. We also review basic aspects of ISM structure accessible to extragalactic observations. Finally, we describe variations in ISM content and star-formation activity among local universe galaxies.

Keywords: Extragalactic astronomy (506); Interstellar medium (847); Nebulae (1095); Disk galaxies (391)

Learning Objectives

- Understand the major components of the interstellar medium (ISM) in galaxies.
- Learn how astronomical observations assess the amount and properties of the ISM in galaxies via astronomical observations.
- Learn how the gas in galaxies is structured on scales accessible to observations of other galaxies.
- Understand how the abundance and properties of these ISM components vary from galaxy-to-galaxy.

1 Introduction

The gas and dust between stars in galaxies form the interstellar medium (ISM). This material represents the potential fuel for future star formation, and its contents and physical state play an important role in the growth and death of galaxies. The ISM is multiphase and dynamic in nature, with gas in distinct chemical states and at different temperatures and densities. New stars will form when the gas becomes cold and dense enough to collapse under the influence of gravity. In the long term, this star formation activity is fueled by the accretion of new ISM material from the surrounding circumgalactic medium (CGM) and the intergalactic media (IGM), the “cosmic web” which is the ultimate repository of new material for galaxy growth. Once inside the galaxy, gas moves under the influence of the galactic potential, its own self-gravity, and the impact from “feedback.” This feedback is energy, momentum, and mass injected by stars and accreting black holes. It heats and reshapes the ISM, while also potentially changing its phase and chemical makeup. Stars also create heavy elements, which are returned to the ISM via stellar winds and various stellar death scenarios including supernova explosions. A significant fraction of these heavy elements are depleted from the gas and form into a solid phase, referred to as dust.

The gas and dust in galaxies also exert a large influence on how we perceive the Universe. Dust on average reprocesses $\geq 50\%$ of the optical and ultraviolet (UV) starlight into infrared (IR) emission. Both absorption and emission lines are also visible from X-ray to radio wavelengths. Some of these represent important channels for the gas to cool, and many of them carry critical information on the heavy

element abundances and physical properties of the gas.

The goal of this chapter is to survey the basic contents of the ISM in galaxies, and to describe standard methods for observing this gaseous material and assessing its physical state. We focus on this in Section 2, which makes up the bulk of the chapter. Then in Section 3 we discuss how this interstellar material is distributed within galaxies at the scales accessible to extragalactic observations. The actual ISM content of galaxies, including the abundance of cold gas and dust, varies from galaxy to galaxy. For example, the ISM in our Milky Way makes up about 10% of the baryonic mass of the galaxy, while in the nearby Small Magellanic Cloud, the ISM makes up $\approx 50\%$ of the total material. These variations follow regular patterns and we describe some of the most important ones in Section 4.

We aim this chapter at a beginning graduate or upper level undergraduate student. As such, we emphasize a first-order, often schematic picture and provide references to recent review articles and textbooks. There an interested reader can dive into these topics in more depth. Also note that this chapter focuses on the contents, structure, and patterns of “low redshift” galaxies, meaning those seen in the nearby, present day universe. One of the most exciting developments of the last two decades has been the emergence of a rich set of observations capturing the gas in galaxies out to Cosmic Dawn. The physics and basic components of the ISM in galaxies do remain the same across cosmic time, but the balance of components evolve. Unfortunately, this is too much to capture in a single article, and we refer interested readers to Tacconi et al. (2020) as an excellent reference for the evolution of gas across cosmic time.

2 Components of the interstellar medium in low redshift galaxies

2.1 Neutral atomic gas

Most of the gas in most star-forming galaxies, including our own Milky Way, is atomic gas, often referred to as H I. In this phase, the hydrogen exists in neutral, atomic form. Atomic gas in galaxies exhibits a wide range of temperatures, $T \approx 50$ K to $T > 5,000$ K, and a correspondingly large range of densities, $n \sim 0.1\text{--}100\text{ cm}^{-3}$. Kalberla and Kerp (2009) and McClure-Griffiths et al. (2023) review the content and structure of the atomic gas in the Milky Way. Our Galaxy harbors $\approx 8 \times 10^9 M_\odot$ of this atomic gas, with a typical surface density $\Sigma_{\text{gas}} = 8 M_\odot \text{ pc}^{-2}$. The H I makes up $\approx 10\%$ of the Milky Way’s total baryonic mass of $\approx 10^{11} M_\odot$, and a majority ($\approx 2/3$) of the total gas mass. In addition to contributing a large fraction of the mass, the H I fills a large fraction of the volume in galaxies. Atomic gas is visible along every line of sight from the Solar System through the Milky Way galaxy.

The atomic gas exists largely in two phases. There is a cold, dense phase referred to as the cold neutral medium, or CNM, which has temperature $T \sim 50\text{--}100$ K, and hydrogen volume density $n \sim 10\text{--}30\text{ cm}^{-3}$. There is also a warm, diffuse phase, referred to as the warm neutral medium or WNM, which has higher temperature $T \sim 6,000\text{--}10,000$ K and lower density $n \sim 0.5\text{ cm}^{-3}$. This warm component of the atomic medium fills a substantial portion of the volume in the disks of galaxies, $\sim 50\%$ in the Solar Neighborhood, and is probably intermixed with a diffuse ionized phase (§2.3). Meanwhile, the cold, dense phase is concentrated into denser structures, and more associated with star formation and molecular material.

The two phases exist in approximate pressure equilibrium, meaning that the product of n and T will be the same for the WNM and CNM. They share a typical thermal pressure $P/k_B = nT \approx 3,500\text{ cm}^{-3}\text{ K}$ in the Solar Neighborhood. This pressure varies across galaxies, and is lower in low density outer regions of galaxy disks or low mass galaxies. Gas with intermediate temperatures and densities between the CNM and WNM has been observed and is sometimes labeled the “unstable neutral medium” (UNM). This likely reflects material recently driven out of thermal equilibrium, e.g., by turbulence or stellar feedback, and is more abundant in lines of sight at high Galactic latitude.

The 21-cm line: H I can be directly observed using radio telescopes in $\lambda = 21\text{-cm}$ line emission (van de Hulst, 1945; Ewen and Purcell, 1951). This “spin flip” hyperfine transition at $\nu = 1.42040580$ MHz ($\lambda \approx 21$ cm) has a low Einstein A , and because of its low energy the condition $h\nu \ll kT$ is fulfilled for all reasonable ISM temperatures. As a result, the two available states are almost always populated according to their statistical weights, i.e., in 3-to-1 ratio. Because the level populations are effectively known, when the 21-cm line is optically thin its intensity can be translated directly to a column density, i.e., a number of H atoms per unit area. Similarly, a measured 21-cm flux from a source at a known distance can be translated into a total mass of H I via $N_{\text{HI}} = 1.823 \times 10^{18}\text{ cm}^{-2} \left(\frac{\int T_{B,\text{HI}} dv}{1\text{ K km s}^{-1}} \right)$ with $\int T_{B,\text{HI}} dv$ the line-integrated 21-cm intensity in brightness units (e.g., Draine, 2011; Condon and Ransom, 2016).

The 21-cm line has been surveyed across the sky by increasingly powerful radio telescopes since the first extragalactic detections by Kerr et al. (1954) (e.g., Fig. 4). The large single dish Arecibo telescope conducted many of the current field-leading surveys of integrated H I content from galaxies, while Very Large Array and Westerbork Synthesis Radio Telescopes (both radio interferometers) made major contributions to our knowledge of the structure of atomic gas in galaxies. In the present landscape, the new Five-hundred-meter Aperture Spherical Telescope (FAST), the MeerKAT and ASKAP arrays, and — in the future — the Square Kilometer Array and Next Generation Very Large Array are all powerful observatories where observing atomic gas via the 21-cm line represents an important part of the science mission.

Other ways to trace the neutral atomic gas: The UV Lyman α line (which is the $n = 2 \rightarrow 1$ electronic transition of hydrogen) can be seen in absorption against background stars and quasars. Such observations have been critical to map out the extended structure of galaxies and the circumgalactic medium. Electronic transitions of other species with appropriate ionization potentials, for example sodium, are also used to trace the presence of atomic gas. Infrared fine structure lines, including the important [Cu] cooling line at $\lambda = 157.7\mu\text{m}$, also emerge from the atomic phase of the ISM. And dust (see below) is mixed with atomic gas, so that the H I can be traced by extinction or dust emission mapping. Because most of these techniques require challenging space-based observations, favorable geometries, and often-uncertain corrections for excitation, abundance, or other factors, they mostly play a complementary role to 21-cm studies.

Separating the phases: The 21-cm line offers a straightforward, reliable way to trace the mass of atomic gas, but does not on its

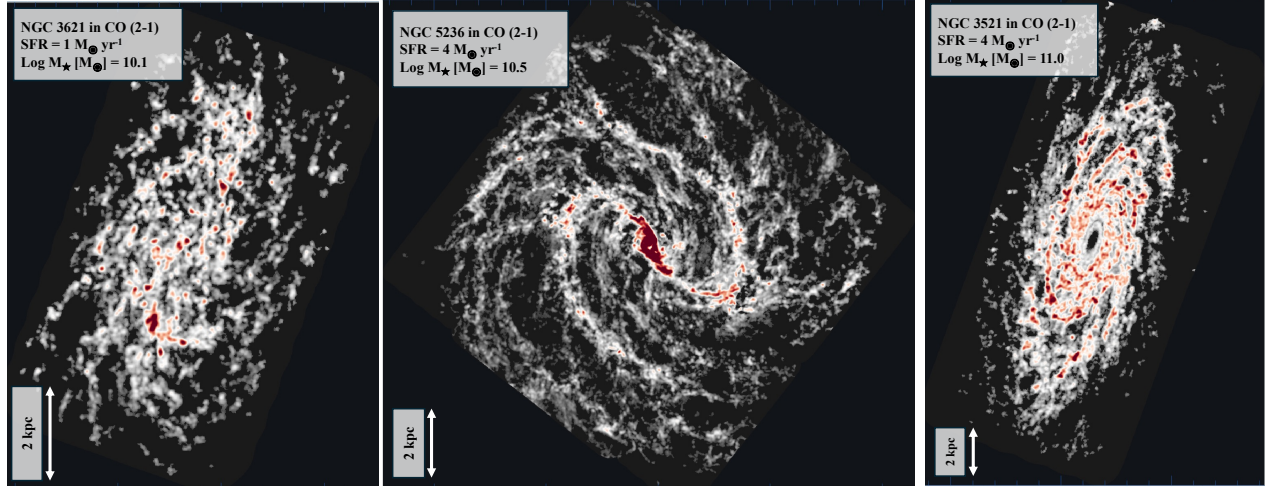


Fig. 1: CO (2-1) maps tracing the molecular gas in three local universe galaxies (Section 2.2). The gas in the molecular phase is cold, mostly $T < 50$ K, shows a wide range of densities, $n_{\text{H}_2} \sim 10^2 \text{ cm}^{-3}$ to $\gtrsim 10^5 \text{ cm}^{-3}$. This gas is observed via rotational line emission of the second most common molecule, CO. The gas is concentrated mostly into giant molecular clouds, visible here as clumps in the CO map. The galaxies here show diverse large scale morphologies: Flocculent structure dominates NGC 3621 (left). In NGC 5236 (M83), strong spiral arms end at a stellar bar, which funnels material to a bright central molecular zone (middle). The massive NGC 3521 lacks molecular gas in the inner bulge and shows spiral structure at larger radii (right). Data from PHANGS–ALMA (Leroy et al., 2021).

own distinguish easily between cold, dense material (CNM) and warm, diffuse material (WNM). In the Milky Way, separating the CNM from the WNM is typically done by contrasting 21-cm absorption observations towards a bright background source with nearby emission. Combining emission and absorption constrains the optical depth of the 21-cm line, the column density of H I, and the spin temperature of the gas (see review in McClure-Griffiths et al., 2023). In the Milky Way, such studies reveal that about 60% of the total 21-cm emission is due to the WNM (Heiles and Troland, 2003). Finding appropriate bright background sources behind other galaxies is challenging, so observational constraints on the balance of phases beyond the Local Group remain weak. It is possible to use the H I line width or morphology in well-resolved observations, or use the [C II] far infrared emission (preferentially emitted by the CNM) to establish the contribution from each phase. This remains an important area for future work.

2.2 Molecular gas

The molecular phase of the ISM consists of mostly cool ($T \approx 10\text{--}100$ K), dense ($n_{\text{H}_2} \approx 10^1\text{--}10^5 \text{ cm}^{-3}$ or more) gas in which the dominant phase of hydrogen is molecular, H_2 . In order for H_2 to become the dominant form of hydrogen, the gas must reach reasonably high densities and be shielded from dissociating UV radiation by a mixture of dust and self-shielding. This self-shielding occurs when dissociating photons are absorbed in discrete transitions, for H_2 the Lyman and Werner bands, that are optically thick because of the high abundance of the molecule; the high optical depth effectively reduces the photodissociation rate, protecting the molecule. As a result of these requirements, molecular gas is typically associated with high column densities, $N(\text{H}) \gtrsim 10^{21} \text{ cm}^{-2}$, and line of sight dust shielding of $A_V \gtrsim 1$ mag (see Wolfire et al., 2022).

In contrast to the volume-filling atomic gas, the molecular gas mass is organized into dense structures that occupy a relatively small volume. These are often referred to as giant molecular clouds (GMCs). These structures are observed to be highly turbulent, with supersonic motions; their typical observed velocity dispersions are $3\text{--}10 \text{ km s}^{-1}$ compared to sound speeds $\ll 1 \text{ km s}^{-1}$. Each cloud also exhibits a wide range of densities and rich substructure (e.g., Heyer and Dame, 2015; Hacar et al., 2023). The densest substructures within molecular clouds, with densities $n_{\text{H}_2} \gtrsim 10^5 \text{ cm}^{-3}$, are often the ones observed to be directly associated with star formation. The mean properties of molecular clouds vary, but typical values are gas mass $M_{\text{gas}} \gtrsim 10^5 M_\odot$, size $10\text{--}100 \text{ pc}$, and surface density $\Sigma_{\text{gas}} \gtrsim 100 M_\odot \text{ pc}^{-2}$ or $N(\text{H}) \gtrsim 10^{22} \text{ cm}^{-2}$ (see reviews in Fukui and Kawamura, 2010; Heyer and Dame, 2015; Schinnerer and Leroy, 2024).

Tracing molecular gas mass using CO line emission: Because its lowest rotational transitions require > 100 K to excite, molecular hydrogen, H_2 , is difficult to observe directly at the temperatures found in molecular clouds. Fortunately, the CO molecule does emit readily under typical conditions found in molecular clouds. CO is the second most abundant molecule, typically $\sim 10^{-4}$ times as abundant compared to H_2 , and represents dominant repository of gas-phase carbon within the molecular gas. The rotational transitions of CO are among the brightest emission lines from galaxies in the mm-wave part of the spectrum. The $J = 1 \rightarrow 0$, $2 \rightarrow 1$, and $3 \rightarrow 2$ CO lines can be observed from the ground by telescopes including the ALMA, the IRAM facilities, the SMA, Nobeyama, and APEX. As a result, CO line emission has become the most common way to trace the distribution and kinematics of molecular gas in galaxies (e.g., Fig. 1).

These CO lines can also be used to trace the molecular gas mass. Doing so relies on a theoretically and empirically calibrated CO-to- H_2 conversion factor, often referred to as X_{CO} or α_{CO} . This conversion factor is essentially a mass-to-light ratio that relates CO intensity to column density of H_2 and/or CO luminosity to total molecular gas mass. Bolatto et al. (2013) review the physics of the CO-to- H_2 conversion

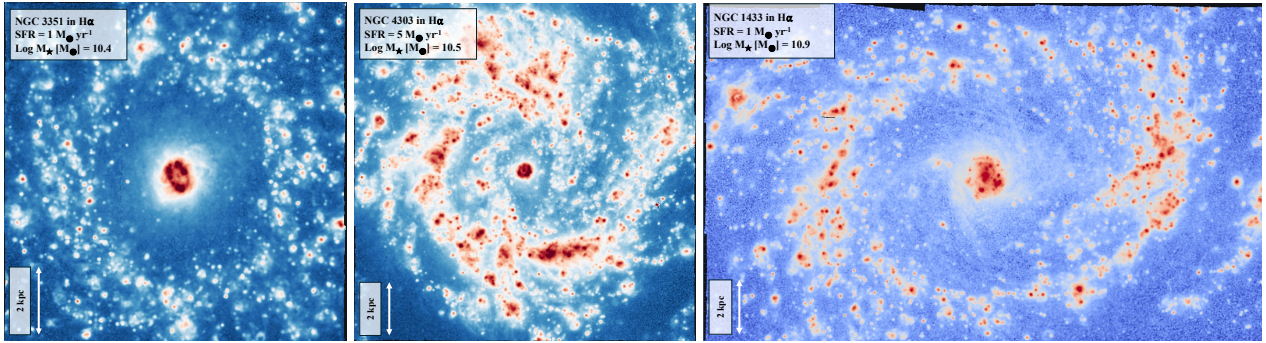


Fig. 2: $H\alpha$ line emission maps tracing the warm ionized gas and production of ionizing photons in three galaxies. The maps show $H\alpha$ recombination line emission, with the brightest clumps corresponding to individual HII regions powered by massive, young stars. In between the HII regions extended, fainter emission traces the diffuse ionized gas, also called the warm ionized medium (Section 2.3). In addition to revealing the distribution of ionized gas, the recombination line flux traces the production of ionizing photons, which in turn traces the mass of massive young stars and the rate of star formation (Section 2.6). These $H\alpha$ maps are from the optical IFU survey PHANGS-MUSE (Emsellem et al., 2022). IFU surveys observe a rich suite of additional optical lines that can be paired to constrain the ionized gas density, temperature, extinction, ionization parameter, and powering source along each line of sight. Ionized gas associated with bar-fed central molecular zones are present at the center of each of these targets.

factor in detail (see also Solomon and Vanden Bout, 2005; Schinnerer and Leroy, 2024). The conversion factor is known to increase at low metallicities, where a “CO-dark” molecular gas phase becomes an important consideration. In such phase, much of the gas is H_2 but CO is comparatively less abundant due to the lack of heavy elements and dust. Meanwhile the CO-to- H_2 conversion factor is lower in the centers of strongly barred spiral galaxies like the Milky Way and in merging galaxies. This reflects lower opacity in the CO, higher temperatures, and (for the higher J CO lines) more excited CO molecules. Research on interpreting CO emission remains an active topic, and the precision with which molecular gas mass can be estimated from CO emission still limits many analyses.

Other ways to trace molecular gas: In addition to CO emission, dust emission and extinction or reddening have been widely used to trace molecular gas (see Section 2.5). Molecular hydrogen can be observed via UV absorption lines, but the need to observe UV background sources through high extinction molecular gas makes this technique challenging to apply to giant molecular clouds. Diffuse gamma ray emission, X-ray, and emission from other molecules, including OH or the subset of warm H_2 that emits in the infrared, have all also been used to trace molecular gas. Because the observations and/or analysis for many of these techniques remain challenging, they are still primarily used to calibrate the more readily observed CO and dust emission. See Bolatto et al. (2013) for more.

Physical conditions from molecular spectroscopy: Molecular spectroscopy beyond only the ^{12}CO lines offers powerful tools to constrain the excitation, temperature, density, opacity, and abundance of specific molecular species in the gas of other galaxies (see reviews of techniques in Shirley, 2015; Mangum and Shirley, 2015). These physical conditions are critical to understanding the nature and fate of the molecular gas. For example, the density of the gas sets the rate at which it will form stars, while the temperature and opacity of the gas help determine the CO-to- H_2 conversion factor. Extragalactic observations can also access a number of relatively bright transitions associated with common molecules that have high Einstein A values and high critical densities. These include the low J lines of HCN, HCO^+ , CS, CN, all of which can be used to trace the balance between dense, excited gas and bulk gas. They are > 10 times fainter than the ^{12}CO rotational lines, and as a result the observations needed to infer density, excitation, or optical depth are more challenging. Even fainter transitions extending throughout the mm- and cm-wave part of the spectrum — including transitions of N_2H^+ , ammonia (NH_3), formaldehyde, SiO, and others — provide a rich set of diagnostics, tracing temperature, density, the presence of shocks, etc. Many of these have been observed in individual sources, but their promise as general tools to studying in other galaxies mostly relies on future facilities like the Next Generation Very Large Array or an upgraded version of ALMA.

2.3 Warm ionized gas

Young, UV-bright stars, active galactic nuclei (AGN), and shocks all ionize interstellar hydrogen, creating a warm ($T \approx 5,000\text{--}15,000$) ionized medium where the dominant form of hydrogen is ionized HII . Concentrations of this ionized gas surround young, massive stars as “ HII regions,” and these tend to be among the most visible ionized gas clouds in galaxies (see Figure 2).

Outside these visible nebulae, a lower density extended component of warm ionized gas pervades galaxies (Haffner et al., 2009; Kewley et al., 2019; Belfiore et al., 2022). This extended ionized gas is referred to as the warm ionized medium (WIM) or diffuse ionized gas (DIG). The DIG contains much more mass than the HII regions, but appears much fainter than HII in line emission because the brightness of ionized gas emission lines is frequently proportional to the emission measure, which depends on the density of the gas squared, $EM \propto \int n^2 dl$. In the Milky Way, the DIG has mass $\sim 2 \times 10^9 M_\odot$, comparable to the mass of the molecular component. This gas is photoionized, and in star-forming galaxies the photoionization source for the DIG is likely dominated by ionizing radiation escaping HII regions around young stars through pre-ionized channels. Other contributors are evolved stars and intermediate age binary systems, which are likely dominant in non-star-forming galaxies.

Hydrogen recombination lines: Ionized hydrogen recombines, with electrons becoming bound to protons. This produces bright line emission that traces the ionized gas in galaxies. The $n = 3 \rightarrow 2$ Balmer α transition, $H\alpha$, is among the brightest optical emission lines from galaxies (e.g., Fig. 2). Other Balmer lines are visible through the optical, while the Paschen, Brackett, and fainter Humphreys and Pfund series are visible in the near-infrared (Osterbrock and Ferland, 2006, is the classic textbook on this topic).

These recombination lines trace the location of ionized gas, but they do not trivially trace its mass because their intensity is proportional to the $EM \sim n^2$. However, because in equilibrium the rate of photoionization equals the rate of recombinations, optical and near-infrared recombination lines are excellent tracers of the ionizing photon production rate. Because most ionizing photons in star-forming galaxies originate from young, massive stars (when not in the presence of a nearby active galactic nucleus), these lines serve as critical tracers of the recent star formation rate (Section 2.6).

To do this, it is important to accurately account for the impact of dust extinction. Fortunately, given temperature and density of the gas the ratios among the hydrogen recombination lines at different wavelengths are known (e.g., Hummer and Storey, 1987; Osterbrock and Ferland, 2006). Observations of recombination lines at widely spaced wavelengths, along with an assumed (or known) extinction curve, yields an estimate of the attenuation towards a HII region. Combining many such lines can help constrain the extinction law and/or the source geometry (Calzetti et al., 1994, 2000).

Physical diagnostics via emission line ratios: Beyond hydrogen recombination lines, warm ionized gas produces a rich spectrum of UV, optical, and near-infrared emission lines. From ratios among the emission lines, e.g., of carbon, oxygen, sulfur, argon, and other abundant elements, one can infer the pressure, volume density of electrons, ionization parameter (a measure of radiation field strength divided by density), and temperature (see review by Kewley et al., 2019).

Optical, UV, and IR line ratios also constrain metallicity, the abundance of heavy elements. Metallicity is often reported as $12 + \log_{10} O/H$, with O/H the abundance of oxygen by number (the Solar abundance $12 + \log_{10} O/H = 8.7$ is frequently also taken as the Solar Neighborhood abundance). The buildup of the elements over time is a crucial topic which has received significant attention, with a variety of methods deployed for different signal-to-noise regimes and types of galaxies (see reviews in Kewley et al., 2019; Sánchez, 2020; Maiolino and Mannucci, 2019). Measuring abundances precisely is challenging, and the exact results often depend on the methodology adopted (Kewley and Ellison, 2008).

Ratios among emission lines from ionized nebulae can also be used to diagnose the nature of the source exciting the emission. BPT-type diagrams (Baldwin et al., 1981; Veilleux and Osterbrock, 1987; Cid Fernandes et al., 2010) separate nebular emission likely to reflect conditions typical of HII regions powered by young massive stars from those powered by shocks and harder radiation fields. This allows one to separate regions dominated by active galactic nuclei, but also large-scale shocks or even more extreme stellar populations (Kewley et al., 2019; Sánchez, 2020).

Optical emission lines can be observed from the ground and so have been studied for many years. Most major ground-based facilities have spectroscopic capabilities, but for many years studies of ionized gas were limited to spectra from individual slits or fibers. A major advance in the last 20 years has been the deployment of wide area “integral field units” that create optical spectroscopic maps, often covering a large portion of the spectrum with many key emission lines for every location across large parts of galaxies. The ATLAS^{3D}, CALIFA, SAMI, and MaNGA surveys (Cappellari et al., 2011; Sánchez et al., 2012; Croom et al., 2012; Bundy et al., 2015), as well as the Multiobject Spectroscopic Explorer (MUSE) on the VLT have played prominent roles (Bacon et al., 2010).

2.4 Hot ionized gas

Hot, low density gas also fills a large volume in the interstellar medium of galaxies, including the immediate region around the Sun. Though it contributes only a modest amount of the overall ISM mass, it fills a significant fraction of the volume and is important to the topology and evolution of the ISM. For example, the hot gas can be associated with pre-ionized channels through which ionizing radiation escapes HII regions. In normal star forming galaxies, this hot gas is shock-ionized by stellar feedback, especially supernova explosions. The earliest stages of supernova feedback are visible as supernova remnants (e.g., Green, 2014), which appear in the X-Ray, optical, and radio emission. These last only a relatively short time, $\lesssim 50,000$ yr, however, and so tend to be less numerous than HII regions (Long et al., 2022; Li et al., 2024).

The hot gas is visible in emission as soft ~ 0.1 – 0.5 keV X-Ray emission, corresponding to temperatures of one to a few million Kelvin (0.1 keV $\approx 1.16 \times 10^6$ K). Lower, but still high (few 10^5 K), temperature gas is also visible in Milky Way absorption studies (e.g., Bowen et al., 2008) but hard to access within the disks of other galaxies. The X-Ray emission from the hot ionized gas in normal galaxies is faint compared to the sensitivity of existing X-Ray facilities. As a result, only a handful of mostly very nearby galaxies have high quality published maps of diffuse X-Ray emission from the disk itself (e.g., Wang et al., 2021; Lopez et al., 2023), though studies of X-Ray visible halos and the CGM have been more common. When sufficient signal to noise can be achieved, X-ray spectroscopy can reveal the temperature, density, and column density of foreground absorbing material. This makes next generation X-Ray facilities with sensitivity to soft X-rays powerful probes of a less-studied phase of the ISM.

2.5 Interstellar dust

Solid grains of interstellar dust pervade galaxies alongside interstellar gas. In the Solar Neighborhood, this dust has mass $\sim 1\%$ the mass of gas. Refractory elements are heavily depleted from the gas phase into the dust, which encompasses as much as 40% of the C and O and even larger fractions of Mg, Si, and Fe (see Draine, 2011; Galliano et al., 2018a). Despite its modest mass, dust plays a crucial role in many aspects of gaseous ISM, including heating, shielding, and chemistry. It is also highly visible through the infrared and submillimeter parts of the spectrum and exerts a strong influence on the emergent optical and UV light from galaxies. Galliano et al. (2018a) and Hensley and

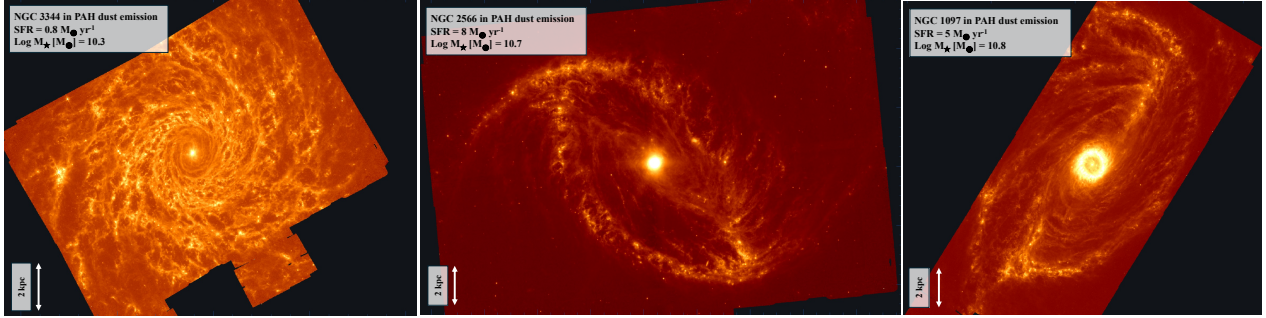


Fig. 3: Emission from polycyclic aromatic hydrocarbon (PAH) dust grains observed by JWST in three galaxies. Interstellar dust contains about half the metals and $\sim 1\%$ of the ISM mass in a galaxy like the Milky Way. It pervades galaxies, mixed with the gaseous phase of the ISM. The emission from dust reflects a mixture of the dust column density and the interstellar radiation field, which heats the dust. Here the same arms, flows along bars, and clouds visible in Fig. 1 are visible in the glow of dust grains. The PAH emission seen here reflects stretching and bending modes of PAH molecules, which produce broad features that dominate the mid-infrared spectrum of galaxies. Observations described in Chown et al. (2024).

Draine (2021) provide overviews of dust in nearby galaxies, including a synthesis of key observations of the Milky Way and Magellanic Clouds.

Observing dust in emission: Dust under typical interstellar conditions emits at infrared wavelengths, from $\sim 3\text{--}1000\mu\text{m}$. At typical ISM densities, $\lesssim 10^5\text{ cm}^{-3}$, the temperature of the larger interstellar dust grains is set by an equilibrium between radiative cooling and radiative heating by the interstellar radiation field (ISRF). An ISRF similar to that in the Solar Neighborhood leads to equilibrium dust temperature $T_{\text{dust}} \approx 20\text{ K}$. This places the peak of the dust spectral energy distribution in the far infrared, $\lambda \approx 100\text{--}250\mu\text{m}$. Observing these wavelengths requires a telescope in space, or at least above most of the atmosphere. IRAS, then ISO, *Spitzer*, *Herschel*, SOFIA, and *Akari* all made critical contributions to our understanding of far infrared emission from dust in galaxies, though there is no operational far infrared facility at this time.

Changes in intensity of the ISRF are often written as U , where $U = 1$ corresponds to the Solar Neighborhood intensity. Taking into account the wavelength-dependent emissivity of grains leads to $T_{\text{dust}} \propto U^{1/6}$. The ISRF is not directly observable, but the dust spectral energy distribution can be observed and T_{dust} inferred from observations at multiple wavelengths that span the peak of the SED. This makes estimating T_{dust} among the most practical methods of estimating the strength of the ISRF in the cold and neutral parts of the ISM.

Once the temperature is known, the optical depth of dust can be modeled. Physical dust models informed by observational constraints give the mass absorption coefficient, κ , which can be used to convert from the optical depth to the mass surface density of dust, Σ_{dust} . This can be compared to measurements of the gas mass to determine the dust-to-gas ratio. Alternatively, if the dust-to-gas ratio is known (or can be estimated), Σ_{dust} can serve as an ISM tracer.

Observing dust in absorption: The properties and distribution of dust in galaxies can also be inferred from its effect on UV, optical, and even near-infrared light. Absorption and scattering by dust extinguishes light by a magnitude difference that depends on wavelength, $\Delta m = -2.5 \log(F_{\text{obs}}/F_{\text{emit}}) = -2.5 \log(e^{-\tau})$, where τ is the dust optical depth. This is the so-called “general extinction” $A_{\lambda} = 1.086\tau_{\lambda}$. The most common approach is to observe interstellar reddening (also called “selective extinction”), which is the difference between two extinctions, $E(\lambda_1 - \lambda_2) = A_{\lambda_1} - A_{\lambda_2}$. Extinction decreases as λ increases, tending to zero when the wavelength is much larger than the dust grain size. Extinction as a function of wavelength (the “extinction curve”) is characterized by the dimensionless parameter $R_V = A_V/E(B - V)$, where B and V are the usual optical photometric bands. Extinction curves measured in the Milky Way can be parameterized so that R_V describes them completely (Cardelli et al., 1989; Fitzpatrick, 1999; Gordon et al., 2023). The R_V ranges between 2 and 6 with larger values corresponding to denser and/or more extinguished regions, and a representative value is taken to be $R_V \approx 3.1$ (Cardelli et al., 1989). Dust and gas are intermixed, so that for a typical Milky Way dust-to-gas ratio at the Solar circle $N(H) = 5.8 \times 10^{21} E(B - V) \text{ H cm}^{-2} \text{ mag}^{-1}$ where $N(H)$ represents the total column of hydrogen atoms in atomic and molecular form (Bohlin et al., 1978; Rachford et al., 2009). Measurements of the interstellar extinction curve extend to longer wavelengths (Rieke and Lebofsky, 1985; Rosenthal et al., 2000; Gao et al., 2013; Gordon et al., 2023), showing a generally decreasing trend of extinction for increasingly long wavelengths but featuring a large bump at $10\mu\text{m}$ and another (less prominent) at $18\mu\text{m}$, both due to silicates. There are variations in the extinction curve between galaxies, with the most notable variation the strength of the UV extinction bump at 2175 \AA associated with small carbonaceous grains (e.g., Gordon et al., 2003). It is important to appreciate that, when determining extinctions over large areas containing ensembles of sources, both the amount and properties of the dust and the relative geometry of the dust and stellar distributions have an impact on the effective extinction: a screen dust distribution in front of the sources produces different effects from an intermixed dust-stars distribution (Calzetti et al., 1994).

Polycyclic aromatic hydrocarbons, very small dust grains: Polycyclic aromatic hydrocarbons (PAHs) are large molecules composed of several or many interlocked benzene-like carbon rings that on Earth are present in soot. PAHs may comprise up to 15% of all ISM carbon (Draine, 2003; Tielens, 2008; Galliano et al., 2018a). They are the smallest interstellar dust grains, and thought to be the carriers of the prominent mid-infrared spectral features observed at $3.3, 6.2, 7.7, 8.6, 11.3, 12.7$, and $17\mu\text{m}$ in galaxies (sometimes called aromatic features or aromatic infrared bands, AIBs). These features are broad ($\lambda/\Delta\lambda \sim 3 - 10$) and bright, particularly in star-forming galaxies where

they carry up to 20% of the infrared luminosity. The different features are due to stretching and bending modes of C–H and C–C bonds. For example, the $3.3\ \mu\text{m}$ feature (bright in small PAHs) is produced by C–H stretching, the C–C stretching gives rise to the 6.2 and $7.7\ \mu\text{m}$ bands, in-plane bending of C–H causes the $8.6\ \mu\text{m}$ feature, while many of the other features are associated with out-of-plane C–H bending. Ratios between PAH spectral features convey information on the size, structure, and charge of the molecules (Draine and Li, 2001; Draine, 2011; Draine et al., 2021). PAHs are somewhat fragile, and they can be destroyed in hot gas (Micelotta et al., 2010a) and shocks (Micelotta et al., 2010b), although they can also be produced in shocks by shattering of larger dust grains (Jones et al., 1996). They also appear to be destroyed in HII regions produced by massive stars, as the emission from PAHs sharply decreases at the ionized gas boundary (Compiègne et al., 2007; Peeters et al., 2024).

PAHs are at the lower end of a continuum of grain sizes which includes very small, small, and large dust grains (Galliano et al., 2018b). Very small grains are likely aggregates of PAHs and other carbonaceous materials (Draine, 2003). Grains of all sizes, including PAHs, absorb non-ionizing UV and optical light which they re-emit primarily in the infrared (although PAHs may also be responsible for emission in optical bands, see e.g., Witt and Lai, 2020). Only large grains, however, are in equilibrium with the illuminating ISRF, reaching a well-defined stable temperature. Smaller grains, particularly grains under $50\ \text{\AA}$ in size, experience large temperature spikes when they absorb a photon (Draine, 2003). This phenomenon is called “stochastic heating” and causes emission by very small grains at short wavelengths, giving rise to a color temperature that is much higher than the blackbody equilibrium temperature (Sellgren, 1984). The combination of high sensitivity in the mid-infrared with high angular resolution and spectroscopy brought about by the *James Webb Space Telescope* are opening a new window into our understanding of PAHs and their use to image and obtain new diagnostics of the ISM in galaxies (e.g., Fig. 3).

Dust as a tracer of gas and the dust-to-gas ratio: Because dust is mixed with atomic, molecular, and (to some degree) ionized gas, mapping the dust column density also represents a powerful way to also map out the distribution of the ISM. This approach traces both atomic and molecular gas, including any CO-dark molecular gas and atomic gas where the 21-cm line is optically thick. This offers an advantage over 21-cm or CO mapping, and has enabled the use of dust as a tracer of otherwise invisible gas (see Bolatto et al., 2013). Converting from Σ_{dust} or A_V to Σ_{gas} requires knowing the appropriate dust-to-gas ratio. In the Solar Neighborhood, depletion studies place this value at ≈ 1 -to-150 (Draine, 2011; Galliano et al., 2018a). This dust-to-gas ratio varies from galaxy to galaxy and within galaxies as we discuss below (Section 4.2).

2.6 Forming stars

Star formation is closely linked to the ISM in galaxies, and recent or ongoing star formation is often traced by observations of the dust and gas (see reviews in Kennicutt and Evans, 2012; Calzetti, 2013). As discussed above, recombination lines provide a powerful, direct probe of the ionizing photon production rate of the young stellar populations powering HII regions. Correcting for the effects of interstellar extinction is critical, and can be done by observing multiple recombination lines at different wavelengths (see above). Radio free-free emission, which is robust to extinction, can also be used to directly trace the ionizing photon production rate in HII regions (e.g., Murphy et al., 2011). Current radio telescopes take significant time to observe the free-free emission from a typical star-forming galaxy, but the Next Generation Very Large Array should be highly efficient at mapping this extinction-free tracer of ionized gas.

Infrared emission is also widely used as a tracer of recent star formation. A large fraction of the dust UV and optical light produced by young stars is absorbed by dust and then re-radiated as infrared emission. This emission can be observed and used to infer the luminosity of the powering population. This approach has more ambiguity than recombination line studies, because the non-ionizing UV and optical emission that give rise to the IR are produced by stars that live over longer timescales than the massive stars producing the ionizing UV, and can be also generated by non-star forming stellar populations. On the other hand, the IR emission is sensitive to newly formed lower mass stars, and is readily available from all-sky imaging by the IRAS and WISE satellites (Wright et al., 2010) and extensive surveys by *Spitzer*, *Herschel*, and now JWST.

In addition to the ISM based methods, the recent (and not-so-recent) star formation rate can be inferred from modeling the stellar population. In more distant galaxies, population synthesis modeling of spectral energy distributions or spectra is the main tool (see reviews in Conroy, 2013; Sánchez, 2020). In closer galaxies, individual stars can be observed and star formation histories reconstructed from their population statistics (e.g., Lewis et al., 2015). Focusing on the most recent star formation, direct counting of recently ($\lesssim 1\ \text{Myr}$) formed young stellar objects, long considered a “gold standard” approach to measuring star formation in the Milky Way, is now possible throughout the Local Group of galaxies thanks to JWST (e.g., Peltonen et al., 2023). Identification and analysis of star clusters represents an intermediate case between resolved stars and integrated light modeling and has also been a powerful tool (Krumholz et al., 2019). Finally, because UV light is mostly generated by young, massive stars, this light on its own has often been used as a tracer of recent star formation (in addition to being folded in to the more sophisticated analyses described above), although large corrections to correct for extinction by dust are necessary in dusty sources.

2.7 Other components

Cosmic rays and magnetic fields are both energetically important but difficult to observe. Cosmic rays contribute significantly to the ISM pressure, are the dominant source of ionization in dust-environmental regions, and may play an important role in driving galactic outflows or fountains (e.g., Thompson and Heckman, 2024). Magnetic fields provide support against gravitational collapse and Galactic observations suggest that they have a role in shaping at least the atomic ISM (e.g., McClure-Griffiths et al., 2023). Both of these phenomena are challenging to study in the Milky Way, and are even harder to access at intergalactic distances. Radio synchrotron emission, which is related to the magnetic field strength among other factors, offers an important probe, and is readily observed at low frequencies (e.g., Condon, 1992).

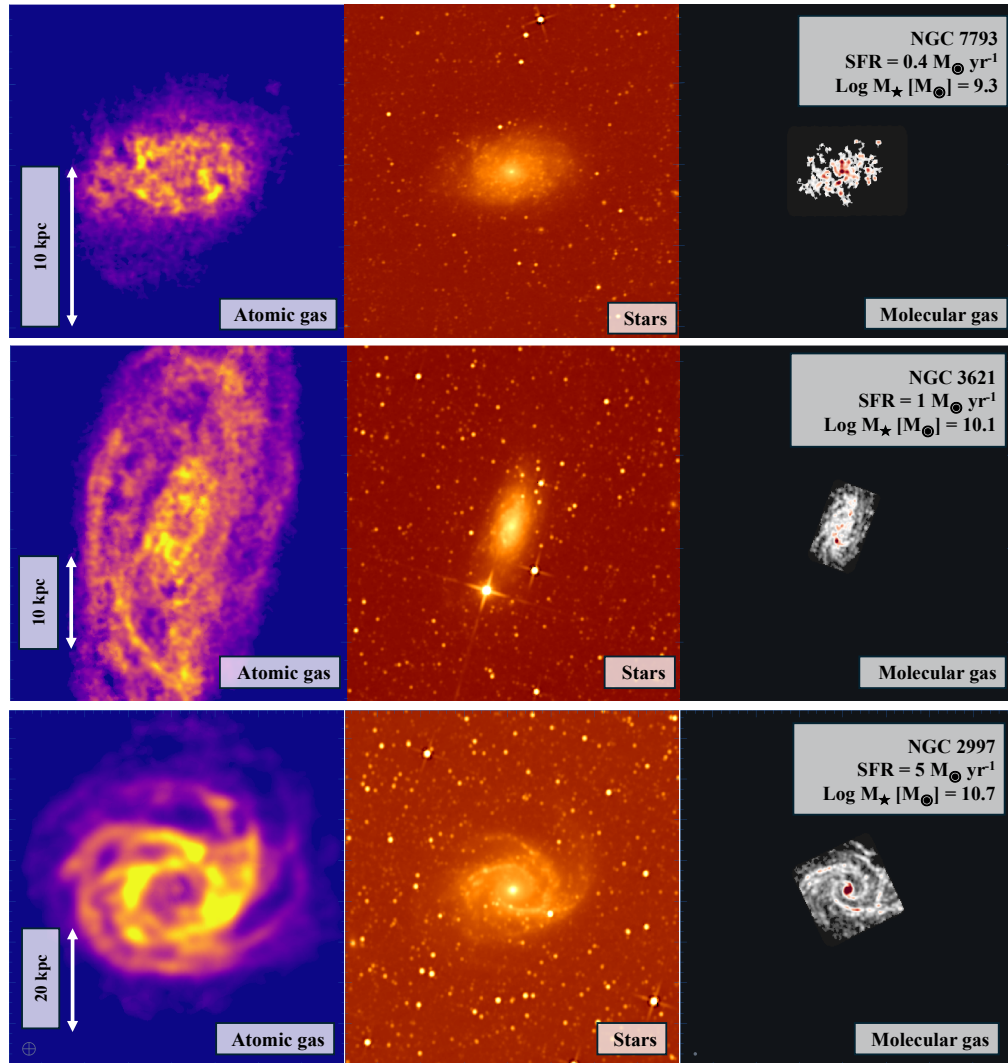


Fig. 4: Wide area view of the atomic gas traced by 21-cm observations (left), near-infrared emission from stars (middle), and CO (2-1) emission tracing molecular gas in three galaxies of different stellar mass. The figure demonstrates the extended atomic gas reservoirs often found in star-forming field galaxies, which can extend well beyond the stellar disk. The colder, denser molecular gas tends to follow the distribution of the stars.

But this emission traces cosmic ray electrons, which are not the energetically dominant component. Magnetic field morphology is accessible through observations of infrared dust polarization and radio synchrotron polarization, but resolution is limited with current instruments and so only a limited number of systems can be studied. Applying new diagnostics of cosmic ray flux and magnetic field strength, including those used in Milky Way studies, to other galaxies will be exciting directions for the next generation of infrared and radio telescopes.

3 Structure of the gas in galaxies

The ISM in galaxies is highly structured. The individual phases show structure on small scales, reflecting gravity, large-scale dynamical features and instabilities, and the balance of heating and cooling, molecule formation and destruction, and so on. On the largest scales, the gas often shows an extended radial distribution that represents the future reservoir for star formation and reflects accretion onto the galaxy by the circumgalactic and intergalactic medium. At intermediate scales, the gas responds to the galactic potential (which is often set by the stellar mass in the inner parts of galaxies) and to heating by stellar feedback. This sets both the vertical distribution of material and drives flows of gas through galaxy disks.

3.1 Cloud-scale structure

Typically, high resolution extragalactic observations targeting nearby targets reach ~ 50 pc resolution. At this resolution, molecular gas appears clumpy and filamentary. Massive concentrations of molecular gas are called giant molecular clouds (GMCs). These appear to be the sites of most massive star formation. Though molecular clouds are not typically well-resolved at extragalactic distances, their sizes span the range 10–100 pc with masses $\gtrsim 10^5 M_\odot$ of H_2 , and they are known to harbor gas at a wide range of densities, $n_{H_2} \sim 10^2$ to $\gtrsim 10^5 \text{ cm}^{-3}$. Their motions are dominated by supersonic turbulence, based on observed line widths that far exceed their thermal line widths. Their kinetic energy, assessed from spectroscopic CO imaging, approximately matches their gravitational potential energy so that they appear at least marginally bound (Heyer and Dame, 2015; Schinnerer and Leroy, 2024). They are frequently viewed as existing in virial equilibrium, though observations also appear consistent with a fast evolving, even collapsing molecular medium (Ballesteros-Paredes et al., 2011).

Emission lines from ionized gas resolve into discrete HII regions at this resolution, as well as a smaller number of supernova remnants and planetary nebulae. These bubbles of ionized gas have sizes ~ 5 –15 pc in Milky Way observations (Anderson et al., 2014), but are often described using a size-luminosity relation (e.g., Wisnioski et al., 2012) that extends to much larger sizes ~ 100 pc in extragalactic observations. They are associated with individual young stellar populations (though not always gravitationally bound clusters), which produce copious amounts of ionizing photons for the first ~ 4 –6 Myr of their lifespan.

Compared to the ionized and molecular gas, the atomic gas appears smooth, though it is worth emphasizing that 21-cm observations typically have significantly worse physical resolution than optical emission line or mm-wave CO observations. Still, observations of Local Group galaxies confirm this idea. HI shows a relatively narrow range of column densities and fills a large fraction of the area in galaxies. The distribution is not perfectly smooth, however. Large-scale shells and holes are often visible in the atomic gas (Bagetakos et al., 2011; Pokhrel et al., 2020) as are dynamical features, including spiral arms. Some of these shells are carved by feedback, though others may naturally result from the flow of gas in the galaxy potential. The drivers of the HI morphology and the density and temperature of the gas filling the HI holes remain active topics of research.

Dust appears mixed with both atomic and molecular gas, and so the column density of dust mirrors the morphology of those components. Because radiation fields are more intense near young stars, the emission from dust near HII regions is enhanced.

At ~ 100 pc resolution these different ISM phases are distinct. Their distributions are correlated on large scales, but not every molecular cloud appears coincident with an HII region, and vice versa (Schruba et al., 2010; Murray, 2011). A common explanation for this decorrelation is that the ISM clouds and star-forming regions are in different evolutionary states. Statistical modeling has been used to infer an evolution sequence for star-forming regions (Chevance et al., 2020; Kim et al., 2022), finding that they evolve quickly likely due to the early impact of stellar feedback (Chevance et al., 2023; Schinnerer and Leroy, 2024).

3.2 Radial structure

The ISM in field star-forming galaxies, as traced by HI observations, often extends to very large galactocentric radius (Wang et al., 2016). The extended atomic gas reservoir in the outer parts of galaxies, which often dominates the galaxy gas mass, frequently has higher surface density than the stellar disk (Bigiel et al., 2010; Wang et al., 2016). The importance of the outer disk HI likely reflects a combination of recently accreted material from the circumgalactic medium Sancisi et al. (2008), and the inability of these extended reservoirs to convert most of their low density atomic gas into the cold, dense gas needed to form stars. Galaxies in dense large scale environments, such as clusters, often show extended HI disks that are truncated or reshaped by interaction with intracluster gas or other galaxies (Cortese et al., 2021). Therefore large scale environment has a significant impact on the atomic gas and overall ISM content of galaxies.

The molecular gas, stellar mass, and star formation activity all tend to follow a more compact distribution than the atomic gas. As a general rule, these three components track one another and follow an approximately exponential profile in star-forming disk galaxies (e.g., Fig. 5 Young and Scoville, 1991; Young et al., 1995; Leroy et al., 2008; Bolatto et al., 2017), though there are important deviations from this trend in both the inner and outer regions of galaxies. The more compact distribution of the molecular gas compared to atomic gas is understood to reflect the high surface density, high gas density, and high interstellar pressure in the inner parts of galaxies, which leads to a higher equilibrium H_2 /HI ratio (Wong and Blitz, 2002; Blitz and Rosolowsky, 2006; Leroy et al., 2008).

3.3 Vertical structure and dynamical equilibrium

Unlike stars, gas is dissipative due to radiative cooling. Therefore, it settles in configurations that follow the potential of the galaxy. In gas-rich spirals, the ISM forms a thin disk, much thinner than the stellar component. In the Milky Way, the vertical distribution of the HI component has an average FWHM of approximately 300 pc, although a better description in the inner Galaxy is two Gaussians with FWHM of 212 and 530 pc (see McClure-Griffiths et al., 2023, and references therein). The thickness flares in the outer galaxy (Levine et al., 2006), following the lower vertical stellar potential. The molecular gas is concentrated on an even thinner layer with FWHM of ≈ 100 pc within the Solar circle (Heyer and Dame, 2015).

The gas in galaxies self regulates to a vertical dynamical equilibrium, in which the weight of the gas is balanced against momentum and energy injected mostly by stellar feedback (Ostriker et al., 2010; Ostriker and Kim, 2022). Because the kinetic energy in the gas will decay on relatively short timescales, the gas will collapse in the absence of such feedback. When the gas begins to collapse it will compress, becoming denser and leading more gas to become molecular and star-forming. This leads to a higher star formation rate, more feedback, and expands the gas in the vertical direction. This expansion lowers the gas density, and therefore also the star formation rate. This negative feedback loop leads to self-regulation that describes the abundance of molecular gas and rate of star formation in galaxies well. The weight of the gas, often expressed as the pressure needed to maintain dynamical equilibrium, can be calculated from observables accessible in face-on galaxies (Ostriker and Kim, 2022; Schinnerer and Leroy, 2024). Although we emphasize the vertical direction, similar self-regulation

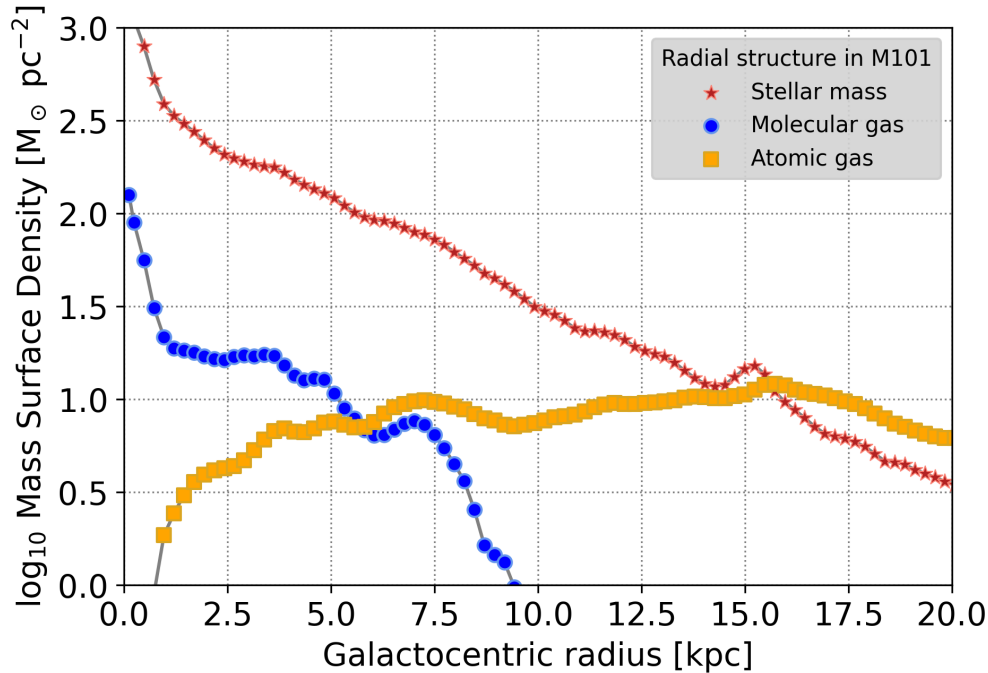


Fig. 5: Example of the radial distribution of mass surface density, measured in solar masses per square parsec, in the massive star-forming spiral galaxy M101. As in Fig. 4 the atomic gas shows an extended distribution with fairly constant mass surface density, while the stellar mass and molecular gas (estimated from CO) fall off exponentially on a shorter length scale. The stellar mass dominates over the ISM in the inner disk, but this situation changes at large galactocentric radii.

has been discussed in the radial direction, often using the Toomre’s Q formalism (e.g., Silk, 1997; Elmegreen, 1997).

3.4 Stellar bars, arms, and nuclear starbursts

Gas also responds to modes in the galactic potential, including spiral arms and stellar bars. Arms concentrate gas into spiral arms, which show much larger fractional enhancements in molecular gas surface density compared to stellar surface density (e.g., Meidt et al., 2021). Debates persist about whether the spirals arms only concentrate gas or also trigger molecular cloud and star formation via shocks or cloud collisions (e.g., Querejeta et al., 2024). In either case, they dominate the visible morphology of many disk galaxies.

Stellar bars also exert a large impact on the gas. Bars are present in $\approx 2/3$ of massive disk galaxies, including our own Milky Way. They drive significant radial gas flows along the bar towards the galaxy center. These flows are visible as dust lanes in optical and UV images and can be seen in emission in CO maps (e.g., Stuber et al., 2023).

Fed by these bar-driven gas flows, molecular gas piles up in the center of many massive disk galaxies. These central molecular zones (CMZs) represent the most common “starburst” environment in the $z = 0$ Universe (Kormendy and Kennicutt, 2004; Schinnerer and Leroy, 2024). They host large amounts of dense molecular gas and high concentrations of star formation activity. These CMZs represent the most prominent sites of super star cluster formation (super star clusters are very massive and compact young star clusters caused by powerful localized star formation events, Portegies Zwart et al., 2010) and frequently are the launching sites for powerful galactic winds (Veilleux et al., 2020; Thompson and Heckman, 2024). Merging or strongly interacting galaxies achieve similar or even more extreme conditions, but are rarer in the present-day universe (Sanders and Mirabel, 1996).

4 Variations in gas content among galaxies

In Sections 2 and 3 we describe a general picture applicable to massive, star-forming $z = 0$ disk galaxies. However, the gas content of galaxies, including the mixture of phases, varies. Much of this variation follows regular patterns. Saintonge and Catinella (2022) provide an excellent review of many of these variations and Tacconi et al. (2020) review how they change as a function of redshift. Kennicutt and Evans (2012) review the relationship between gas and star formation in massive $z = 0$ disk galaxies, and Sánchez (2020) review aspects of structure and scaling relations for $z = 0$ galaxies based on IFU surveys.

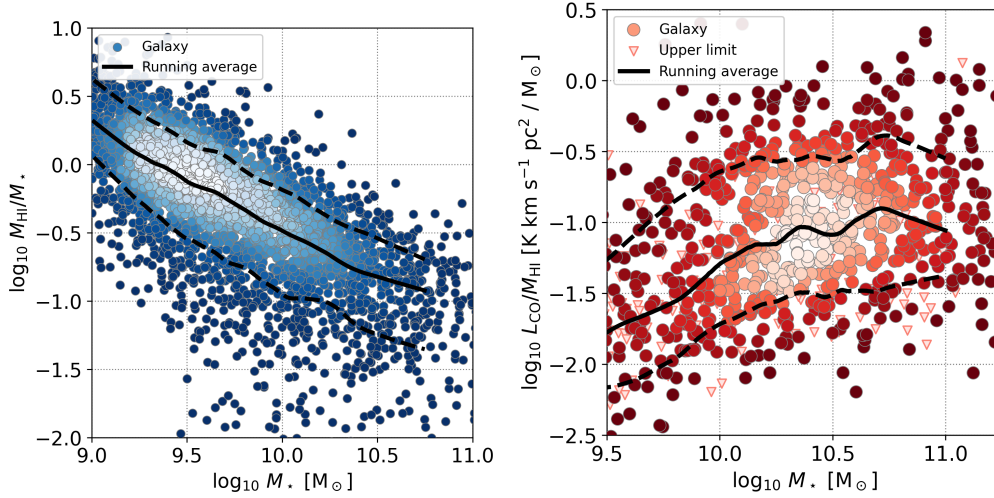


Fig. 6: Illustration of varying ISM content by galaxy mass. Each point here represents one galaxy with an integrated mass measurement from a large compilation drawn heavily from Saintonge et al. (2017) and Colombo et al. (2020) and Makarov et al. (2014). The left panel shows that for star forming galaxies the ratio of atomic gas mass to stellar mass decreases with increasing stellar mass. The right panel shows how the ratio of CO luminosity, tracing molecular gas mass, to atomic gas increases with stellar mass. More massive star-forming galaxies have less fractional mass in their interstellar medium and more molecular compared to atomic gas. Color in the points reflects the density of data in that part of the plot. Upper limits in the right panel show galaxies where CO is not detected.

4.1 Star formation activity, stellar mass, and gas mass

For star-forming disk galaxies, the star formation rate (SFR) of the galaxy correlates with the stellar mass, M_* . This appears to hold true across redshift (e.g., Tacconi et al., 2020), and the relatively tight (rms scatter ≈ 0.3 – 0.4 dex) relation is referred to as the “main sequence of star forming galaxies.” “Starburst” galaxies are often defined by having high SFR relative to galaxies with similar stellar mass, and so they reside above the star forming main sequence. Early type galaxies, “green valley” galaxies, or “quenching” galaxies have low SFR relative to that expected for their stellar mass (though note that all of these terms are also laden with additional meaning).

The star formation rate of a galaxy also correlates with the cold gas mass. The ratio of the two quantities expresses the “specific” star formation rate per unit gas, which is sometimes referred to as the star formation efficiency of the gas, $\text{SFR}/M_{\text{gas}}$ (Young and Scoville, 1991; Young et al., 1996). Alternatively this quantity is expressed as the gas depletion time, $M_{\text{gas}}/\text{SFR}$, which expresses the time needed for current star formation to consume the entire gas reservoir. Specifically, the star formation rate of a galaxy tracks the molecular gas mass, as traced by CO (Young and Scoville, 1991; Young et al., 1995; Kennicutt and Evans, 2012; Saintonge and Catinella, 2022), with typical molecular gas depletion times of ≈ 1 – 2 Gyr for galaxies on the star forming main sequence at $z = 0$ (Leroy et al., 2013; Tacconi et al., 2020; Saintonge and Catinella, 2022). On galaxy scales, the star formation rate also correlates with the atomic gas mass, but the depletion time of molecular gas varies less than the atomic gas depletion time, and in studies that resolve galaxy disks, star formation activity correlates with molecular, rather than atomic gas (Bigiel et al., 2008; Leroy et al., 2008; Schruba et al., 2011). Other galaxies thus apparently follow the same situation seen in the Milky Way, where stars form from clouds made of predominantly molecular gas. Because atomic gas represents more of the overall ISM mass in galaxies, this implies that the abundance of molecular gas can represent an important regulating factor in setting the star formation rate.

The Kennicutt Schmidt relation offers a popular alternative framework (instead of SFE or τ_{dep}) to express the relationship between gas and star formation. This approach (Kennicutt, 1989, 1998) considers the surface densities of gas and star formation rate, Σ_{gas} and Σ_{SFR} , as the primary variables and posits a power law relationship, $\Sigma_{\text{SFR}} \propto \Sigma_{\text{gas}}^n$ between them to describe galaxies. Considering atomic and molecular gas combined, the relationship has index $n \approx 1.5$ – 2 for integrated galaxies, depending on the sample studied and treatment of α_{CO} . Reflecting the more direct relationship between molecular gas and star formation, many studies focusing on the molecular gas Kennicutt Schmidt relation. These tend to find $n \approx 0.8$ – 1.3 (Bigiel et al., 2008; Kennicutt and Evans, 2012; Leroy et al., 2013; Sun et al., 2023).

The molecular gas depletion time varies (see reviews in Saintonge and Catinella, 2022; Tacconi et al., 2020). It appears shorter, indicating more efficient star formation, in the dense concentrations of gas found in bar-fed central molecular zones and merging galaxies. It also appears longer in quiescent galaxies, i.e., galaxies that have star formation rates lower than those predicted by the star-forming main sequence. It may also be shorter in low mass galaxies, but this result depends sensitively on still-uncertain knowledge of the CO-to- H_2 conversion factor. Because the star formation occurs in molecular gas, the total or atomic gas depletion time depend to first order on the balance of atomic and molecular gas in the galaxy combined with the molecular gas depletion time.

4.2 Abundance and makeup of the ISM

The mass of ISM material in a galaxy also varies. Most notably, the ratio of ISM mass to stellar mass varies as a function of stellar (or halo or total baryonic) mass for galaxies on the star forming main sequence (e.g., Fig. 6). The sense of this variation is that galaxies with low stellar mass have a higher gas-to-stellar mass ratio. These large gas reservoirs are overwhelmingly H I , so that a low mass star-forming galaxy can have even more mass in an atomic gas ISM than it has in stars (Hunter et al., 2024).

The makeup of the ISM also varies. In star-forming galaxies the mass of molecular gas tracks the stellar mass fairly well (Young and Scoville, 1991; Saintonge and Catinella, 2022). The molecular to atomic gas ratio correlates with stellar mass for star-forming galaxies, this variation has the sense that a massive galaxy like our Milky Way holds a larger fraction of its overall ISM mass in the molecular phase, while lower mass galaxies have more atomic gas compared to molecular gas. A similar correlation exists with stellar surface density (Hunter et al., 1998; Saintonge and Catinella, 2022), and with galaxy morphological type in the direction that later type galaxies tend to have lower ratios of molecular to atomic gas (Young and Knezek, 1989; Obreschkow and Rawlings, 2009). The lower molecular-to-atomic gas ratio in lower mass galaxies is often attributed to the effects of lower metallicity and lower pressure. The former enhances photodissociation of molecules and slows down their formation, while the latter (caused by the lower stellar potential) diminishes the density of the gas and the conversion of H I to H_2 .

Many of these trends are, strictly speaking, trends for the luminosity of a low lying CO rotational transition versus the luminosity of the H I 21 cm transition. While the translation of the latter to atomic gas mass is fairly robust, converting CO luminosity to molecular gas mass is frequently done assuming a constant conversion factor, likely an oversimplification (Bolatto et al., 2013). Although the trends mentioned above will not change qualitatively, the values of their slopes depend on assumptions about the CO-to- H_2 conversion, which is affected by metallicity, velocity dispersion, temperature of the molecular gas, and possibly other environmental parameters such as X-ray and cosmic ray flux (see §2.2).

Metallicity and stellar mass correlate, in the direction of lower stellar mass galaxies being poorer in heavy elements (Tremonti et al., 2004; Maiolino and Mannucci, 2019). This correlation is attributed mostly to lower mass galaxies being less able to retain nucleosynthetic products, which are preferentially lost to the CGM and IGM via enriched galactic winds that escape the shallower potential wells of these galaxies (Tumlinson et al., 2017). The introduction of a third parameter (star formation rate) produces a tighter correlation that shows less evolution with redshift (Mannucci et al., 2010). This is likely caused by the star formation rate acts as a proxy for both the inflow rate of new gas, which is likely relatively pristine and low metallicity and the strength of galactic winds.

Metallicity and dust-to-gas ratio are also strongly correlated (Draine et al., 2007; Rémy-Ruyer et al., 2014; Galliano et al., 2018b). Heavy elements are necessary to make dust grains, and so their abundance affects the gas-to-dust ratio. Though challenging, observations of the dust-to-gas ratio in low metallicity, low mass systems suggest low dust-to-metals ratios. That is, observations suggest that the fraction of heavy elements in the dust phase is lower for low mass, low metallicity galaxies. This can be understood in terms of simple evolutionary models that balance dust production from stars and supernovae, buildup in the ISM, and destruction (e.g., Galliano et al., 2018b; Aniano et al., 2020). Because observations of this trend are technically challenging and sparse, especially robust observations for low metallicity galaxies, the precise behavior of the dust-to-metals ratio at low metallicity ($12 + \log_{10} \text{O/H} \lesssim 8$) remains an important area for future work.

4.3 Mergers, starburst galaxies, quiescent and quenching galaxies

Galaxies that are located over the main sequence (§4.1) display an overabundance of star formation for their stellar mass and are called starbursts. These galaxies are rare, less than 1% of the population depending on the precise definition. The formation activity of starbursts is such that they use up their molecular gas reservoir very quickly, on a timescale that can be as short as ~ 0.1 Gyr compared to a typical 1 – 2 Gyr for galaxies near the star forming main sequence (Tacconi et al., 2020; Saintonge and Catinella, 2022). Some of the most strongly star-forming outliers are the result of equal mass mergers, where the interaction produces torques that remove angular momentum from the gas driving it down the potential well (Sanders and Mirabel, 1996). Interactions among dissimilar mass galaxies can also produce starbursts. The prototypical starburst galaxy M82 is an example of this, where the starburst is caused by its interaction with the much larger nearby spiral galaxy M81. Bars also can drive gas into galaxy centers and give rise circumnuclear starburst as discussed above in Section 3.4.

Starbursts are very gas rich, and are characterized not just by high star formation rates per unit stellar mass but also by high molecular-to-atomic gas ratios, high gas fractions, and short molecular gas depletion times. Much of the star formation activity in starbursts takes place behind large columns of dust. This can make it difficult to study the structure and physical conditions in these systems at optical wavelengths, but also makes these galaxies shine brightly in the infrared. Analysis of the *IRAS* far-infrared satellite data found that some of the local most actively star-forming galaxies were unremarkable at optical wavelengths, but displayed IR luminosities $\gtrsim 10^{12} L_{\odot}$. These objects receive the name of “Ultra-Luminous IR Galaxies” or ULIRGs (Sanders and Mirabel, 1996).

On the other end of the spectrum of activity are quiescent or quenched galaxies. They show low star formation rates for their stellar mass, which places them below the star forming main sequence. These galaxies are usually, but not always, gas poor for both molecular and atomic gas (Saintonge and Catinella, 2022). They also tend to have earlier morphological types, frequently appearing as lenticular or elliptical galaxies. They may display ionized gas emission, but it tends to be low intensity and related to ionization by older stellar populations, hence unrelated to star formation activity (Sánchez, 2020). Some of the remnant neutral and molecular gas in these systems may be stabilized against collapse and subsequent star formation by the stellar potential Martig et al. (2009), so that a galaxy does not need to be completely devoid of cold gas to be quiescent (Colombo et al., 2020; Saintonge and Catinella, 2022). Quiescent galaxies are very abundant in high density environments like galaxy clusters, where gas is removed by interactions with other galaxies and the intra-cluster medium.

5 Conclusions

Even after almost a century of multi-wavelength study, the ISM in galaxies remains a rich topic of critical importance to the growth of structure in the Universe. Current and planned facilities including ALMA, JWST, MeerKAT, the VLA, ngVLA and SKA, and any next generation infrared or X-ray probe missions will be powering new advances each year and promise a bright future. The textbooks by Draine (2011) and Osterbrock and Ferland (2006) are outstanding resources to dive more into this rich topic, while Ryden and Pogge (2021), Condon and Ransom (2016), Tielens (2005), and the classic book by Spitzer (1968) offer accessible introductory texts.

Acknowledgments

This is a pre-print of a chapter for the Encyclopedia of Astrophysics (edited by I. Mandel, section editor S. McGee) to be published by Elsevier as a Reference Module. A.K.L. gratefully acknowledges support by a Humboldt Research Award and grants NSF AST AWD 2205628, JWST-GO-02107.009-A, and JWST-GO-03707.001-A. A.D.B. gratefully acknowledges partial support from grants NSF AST 2108140 and 2307441.

References

- Anderson LD, Bania TM, Balser DS, Cunningham V, Wenger TV, Johnstone BM and Armentrout WP (2014), May. The WISE Catalog of Galactic H II Regions. *The Astrophysical Journal Supplement Series* 212 (1), 1. doi:10.1088/0067-0049/212/1/1. 1312.6202.
- Aniano G, Draine BT, Hunt LK, Sandstrom K, Calzetti D, Kennicutt RC, Dale DA, Galametz M, Gordon KD, Leroy AK, Smith JDT, Roussel H, Sauvage M, Walter F, Armus L, Bolatto AD, Boquien M, Crocker A, De Looze I, Donovan Meyer J, Helou G, Hinz J, Johnson BD, Koda J, Miller A, Montiel E, Murphy EJ, Relaño M, Rix HW, Schinnerer E, Skibba R, Wolfire MG and Engelbracht CW (2020), Feb. Modeling Dust and Starlight in Galaxies Observed by Spitzer and Herschel: The KINGFISH Sample. *The Astrophysical Journal* 889 (2), 150. doi:10.3847/1538-4357/ab5fdb. 1912.04914.
- Bacon R, Accardo M, Adjali L, Anwand H, Bauer S, Biswas I, Blaizot J, Boudon D, Brau-Nogue S, Brinchmann J, Caillier P, Capolani L, Carollo CM, Contini T, Couderc P, Daguisé E, Deiries S, Delabre B, Dreizler S, Dubois J, Dupieux M, Dupuy C, Emsellem E, Fechner T, Fleischmann A, François M, Gallou G, Gharsa T, Glindemann A, Gojak D, Guiderdoni B, Hansali G, Hahn T, Jarno A, Kelz A, Koehler C, Kosmowski J, Laurent F, Le Floch M, Lilly SJ, Lizon JL, Loupias M, Manescau A, Monstein C, Nicklas H, Olaya JC, Pares L, Pasquini L, Pécontal-Rousset A, Pelló R, Petit C, Popow E, Reiss R, Remillieux A, Renault E, Roth M, Rupprecht G, Serre D, Schaye J, Soucail G, Steinmetz M, Streicher O, Stuijk R, Valentin H, Vernet J, Weilbacher P, Wisotzki L and Yelle N (2010), Jul., The MUSE second-generation VLT instrument, McLean IS, Ramsay SK and Takami H, (Eds.), Ground-based and Airborne Instrumentation for Astronomy III, Society of Photo-Optical Instrumentation Engineers (SPIE) Conference Series, 7735, pp. 773508, 2211.16795.
- Bagetakos I, Brinks E, Walter F, de Blok WJG, Usero A, Leroy AK, Rich JW and Kennicutt R. C. J (2011), Jan. The Fine-scale Structure of the Neutral Interstellar Medium in Nearby Galaxies. *The Astronomical Journal* 141 (1), 23. doi:10.1088/0004-6256/141/1/23. 1008.1845.
- Baldwin JA, Phillips MM and Terlevich R (1981), Feb. Classification parameters for the emission-line spectra of extragalactic objects. *Publications of the Astronomical Society of the Pacific* 93: 5–19. doi:10.1086/130766.
- Ballesteros-Paredes J, Hartmann LW, Vázquez-Semadeni E, Heitsch F and Zamora-Avilés MA (2011), Feb. Gravity or turbulence? Velocity dispersion-size relation. *Monthly Notices of the Royal Astronomical Society* 411 (1): 65–70. doi:10.1111/j.1365-2966.2010.17657.x. 1009.1583.
- Belfiore F, Santoro F, Groves B, Schinnerer E, Kreckel K, Glover SCO, Klessen RS, Emsellem E, Blanc GA, Congiu E, Barnes AT, Boquien M, Chevance M, Dale DA, Krujssens JMD, Leroy AK, Pan HA, Pessa I, Schrubba A and Williams TG (2022), Mar. A tale of two DIGs: The relative role of H II regions and low-mass hot evolved stars in powering the diffuse ionised gas (DIG) in PHANGS-MUSE galaxies. *Astronomy & Astrophysics* 659, A26. doi:10.1051/0004-6361/202141859. 2111.14876.
- Bigiel F, Leroy A, Walter F, Brinks E, de Blok WJG, Madore B and Thornley MD (2008), Dec. The Star Formation Law in Nearby Galaxies on Sub-Kpc Scales. *The Astronomical Journal* 136 (6): 2846–2871. doi:10.1088/0004-6256/136/6/2846. 0810.2541.
- Bigiel F, Leroy A, Walter F, Blitz L, Brinks E, de Blok WJG and Madore B (2010), Nov. Extremely Inefficient Star Formation in the Outer Disks of Nearby Galaxies. *The Astronomical Journal* 140 (5): 1194–1213. doi:10.1088/0004-6256/140/5/1194. 1007.3498.
- Blitz L and Rosolowsky E (2006), Oct. The Role of Pressure in GMC Formation II: The H₂-Pressure Relation. *The Astrophysical Journal* 650 (2): 933–944. doi:10.1086/505417. astro-ph/0605035.
- Bohlin RC, Savage BD and Drake JF (1978), Aug. A survey of interstellar H I from Ly α absorption measurements. II. *ApJ* 224: 132–142. doi:10.1086/156357.
- Bolatto AD, Wolfire M and Leroy AK (2013), Aug. The CO-to-H₂ Conversion Factor. *Annual Review of Astronomy & Astrophysics* 51 (1): 207–268. doi:10.1146/annurev-astro-082812-140944. 1301.3498.
- Bolatto AD, Wong T, Utomo D, Blitz L, Vogel SN, Sánchez SF, Barrera-Ballesteros J, Cao Y, Colombo D, Dannerbauer H, García-Benito R, Herrera-Camus R, Husemann B, Kalinova V, Leroy AK, Leung G, Levy RC, Mast D, Ostriker E, Rosolowsky E, Sandstrom KM, Teuben P, van de Ven G and Walter F (2017), Sep. The EDGE-CALIFA Survey: Interferometric Observations of 126 Galaxies with CARMA. *The Astrophysical Journal* 846 (2), 159. doi:10.3847/1538-4357/aa86aa. 1704.02504.
- Bowen DV, Jenkins EB, Tripp TM, Sembach KR, Savage BD, Moos HW, Oegerle WR, Friedman SD, Gry C, Kruk JW, Murphy E, Sankrit R, Shull JM, Sonneborn G and York DG (2008), May. The Far Ultraviolet Spectroscopic Explorer Survey of O VI Absorption in the Disk of the Milky Way. *The Astrophysical Journal Supplement Series* 176 (1): 59–163. doi:10.1086/524773. 0711.0005.
- Bundy K, Bershadsky MA, Law DR, Yan R, Drory N, MacDonald N, Wake DA, Cherinka B, Sánchez-Gallego JR, Weijmans AM, Thomas D, Tremonti C, Masters K, Coccatto L, Diamond-Stanic AM, Aragón-Salamanca A, Avila-Reese V, Badenes C, Falcón-Barroso J, Belfiore F, Bizyaev D, Blanc GA, Bland-Hawthorn J, Blanton MR, Brownstein JR, Byler N, Cappellari M, Conroy C, Dutton AA, Emsellem E, Etherington J, Frinchaboy PM, Fu H, Gunn JE, Harding P, Johnston EJ, Kauffmann G, Kinemuchi K, Klaene MA, Knapen JH, Leauthaud A, Li C, Lin L, Maiolino R, Malanushenko V, Malanushenko E, Mao S, Maraston C, McDermid RM, Merrifield MR, Nichol RC, Oravetz D, Pan K, Parejko JK, Sanchez SF, Schlegel D, Simmons A, Steele O, Steinmetz M, Thanjavur K, Thompson BA, Tinker JL, van den Bosch RCE, Westfall KB, Wilkinson D, Wright S, Xiao T and Zhang K (2015), Jan. Overview of the SDSS-IV MaNGA Survey: Mapping nearby Galaxies at Apache

- Point Observatory. *The Astrophysical Journal* 798 (1), 7. doi:10.1088/0004-637X/798/1/7. 1412.1482.
- Calzetti D (2013), Star Formation Rate Indicators, Falcón-Barroso J and Knapen JH, (Eds.), *Secular Evolution of Galaxies*, pp. 419.
- Calzetti D, Kinney AL and Storchi-Bergmann T (1994), Jul. Dust Extinction of the Stellar Continua in Starburst Galaxies: The Ultraviolet and Optical Extinction Law. *The Astrophysical Journal* 429: 582. doi:10.1086/174346.
- Calzetti D, Armus L, Bohlin RC, Kinney AL, Koornneef J and Storchi-Bergmann T (2000), Apr. The Dust Content and Opacity of Actively Star-forming Galaxies. *The Astrophysical Journal* 533 (2): 682–695. doi:10.1086/308692. astro-ph/9911459.
- Cappellari M, Emsellem E, Krajnović D, McDermid RM, Scott N, Verdoes Kleijn GA, Young LM, Alatalo K, Bacon R, Blitz L, Bois M, Bournaud F, Bureau M, Davies RL, Davis TA, de Zeeuw PT, Duc PA, Khochfar S, Kuntschner H, Lablanche PY, Morganti R, Naab T, Oosterloo T, Sarzi M, Serra P and Weijmans AM (2011), May. The ATLAS^{3D} project - I. A volume-limited sample of 260 nearby early-type galaxies: science goals and selection criteria. *MNRAS* 413 (2): 813–836. doi:10.1111/j.1365-2966.2010.18174.x. 1012.1551.
- Cardelli JA, Clayton GC and Mathis JS (1989), Oct. The Relationship between Infrared, Optical, and Ultraviolet Extinction. *The Astrophysical Journal* 345: 245. doi:10.1086/167900.
- Chevance M, Kruijssen JMD, Hygate APS, Schrub A, Longmore SN, Groves B, Henshaw JD, Herrera CN, Hughes A, Jeffreson SMR, Lang P, Leroy AK, Meidt SE, Pety J, Razza A, Rosolowsky E, Schinnerer E, Bigiel F, Blanc GA, Emsellem E, Faesi CM, Glover SCO, Haydon DT, Ho IT, Kreckel K, Lee JC, Liu D, Querejeta M, Saito T, Sun J, Usero A and Utomo D (2020), Apr. The lifecycle of molecular clouds in nearby star-forming disc galaxies. *Monthly Notices of the Royal Astronomical Society* 493 (2): 2872–2909. doi:10.1093/mnras/stz3525. 1911.03479.
- Chevance M, Krumholz MR, McLeod AF, Ostriker EC, Rosolowsky EW and Sternberg A (2023), Jul., The Life and Times of Giant Molecular Clouds, Inutsuka S, Aikawa Y, Muto T, Tomida K and Tamura M, (Eds.), *Astronomical Society of the Pacific Conference Series*, Astronomical Society of the Pacific Conference Series, 534, pp. 1, 2203.09570.
- Chown R, Leroy AK, Sandstrom K, Chasteney J, Sutter J, Koch EW, Koziol HB, Neumann L, Sun J, Williams TG, Baron D, Anand GS, Barnes AT, Bazzi Z, Belfiore F, Bolatto A, Boquien M, Cao Y, Chevance M, Colombo D, Dale DA, Egorov OV, Eibensteiner C, Emsellem E, Hassani H, Henshaw JD, He H, Kim J, Kreckel K, Meidt SE, Murphy EJ, Oakes EK, Ostriker EC, Pan HA, Pathak D, Rosolowsky E, Sarbadhicary SK, Schinnerer E and Teng YH (2024), Oct. Polycyclic Aromatic Hydrocarbon and CO(2-1) Emission at 50-150 pc Scales in 66 Nearby Galaxies. *arXiv e-prints*, arXiv:2410.05397doi:10.48550/arXiv.2410.05397. 2410.05397.
- Cid Fernandes R, Stasińska G, Schlickmann MS, Mateus A, Vale Asari N, Schoenell W and Sodr   L (2010), Apr. Alternative diagnostic diagrams and the ‘forgotten’ population of weak line galaxies in the SDSS. *MNRAS* 403 (2): 1036–1053. doi:10.1111/j.1365-2966.2009.16185.x. 0912.1643.
- Colombo D, Sanchez SF, Bolatto AD, Kalinova V, Weiß A, Wong T, Rosolowsky E, Vogel SN, Barrera-Ballesteros J, Dannerbauer H, Cao Y, Levy RC, Utomo D and Blitz L (2020), Dec. The EDGE-CALIFA survey: exploring the role of molecular gas on galaxy star formation quenching. *A&A* 644, A97. doi:10.1051/0004-6361/202039005. 2009.08383.
- Compi  gne M, Abergel A, Verstraete L, Reach WT, Habart E, Smith JD, Boulanger F and Joblin C (2007), Aug. Aromatic emission from the ionised mane of the Horsehead nebula. *A&A* 471 (1): 205–212. doi:10.1051/0004-6361:20066172. 0706.1510.
- Condon JJ (1992), Jan. Radio emission from normal galaxies. *Annual Review of Astronomy & Astrophysics* 30: 575–611. doi:10.1146/annurev.aa.30.090192.003043.
- Condon JJ and Ransom SM (2016). *Essential Radio Astronomy*.
- Conroy C (2013), Aug. Modeling the Panchromatic Spectral Energy Distributions of Galaxies. *Annual Review of Astronomy & Astrophysics* 51 (1): 393–455. doi:10.1146/annurev-astro-082812-141017. 1301.7095.
- Cortese L, Catinella B and Smith R (2021), Aug. The Dawes Review 9: The role of cold gas stripping on the star formation quenching of satellite galaxies. *Publications of the Astronomical Society of Australia* 38, e035. doi:10.1017/pasa.2021.18. 2104.02193.
- Croom SM, Lawrence JS, Bland-Hawthorn J, Bryant JJ, Fogarty L, Richards S, Goodwin M, Farrell T, Miziarski S, Heald R, Jones DH, Lee S, Colless M, Brough S, Hopkins AM, Bauer AE, Birchall MN, Ellis S, Horton A, Leon-Saval S, Lewis G, L  pez-S  nchez   R, Min SS, Trinh C and Trowland H (2012), Mar. The Sydney-AAO Multi-object Integral field spectrograph. *MNRAS* 421 (1): 872–893. doi:10.1111/j.1365-2966.2011.20365.x. 1112.3367.
- Draine BT (2003), Jan. Interstellar Dust Grains. *ARA&A* 41: 241–289. doi:10.1146/annurev.astro.41.011802.094840. astro-ph/0304489.
- Draine BT (2011). *Physics of the Interstellar and Intergalactic Medium*.
- Draine BT and Li A (2001), Apr. Infrared Emission from Interstellar Dust. I. Stochastic Heating of Small Grains. *ApJ* 551 (2): 807–824. doi:10.1086/320227. astro-ph/0011318.
- Draine BT, Dale DA, Bendo G, Gordon KD, Smith JDT, Armus L, Engelbracht CW, Helou G, Kennicutt R. C. J, Li A, Roussel H, Walter F, Calzetti D, Moustakas J, Murphy EJ, Rieke GH, Bot C, Hollenbach DJ, Sheth K and Teplitz HI (2007), Jul. Dust Masses, PAH Abundances, and Starlight Intensities in the SINGS Galaxy Sample. *ApJ* 663 (2): 866–894. doi:10.1086/518306. astro-ph/0703213.
- Draine BT, Li A, Hensley BS, Hunt LK, Sandstrom K and Smith JDT (2021), Aug. Excitation of Polycyclic Aromatic Hydrocarbon Emission: Dependence on Size Distribution, Ionization, and Starlight Spectrum and Intensity. *ApJ* 917 (1), 3. doi:10.3847/1538-4357/abff51. 2011.07046.
- Elmegreen BG (1997), May, Theory of Starbursts in Nuclear Rings, Franco J, Terlevich R and Serrano A, (Eds.), *Revista Mexicana de Astronom  a y Astrof  sica Conference Series*, Revista Mexicana de Astronom  a y Astrof  sica Conference Series, 6, pp. 165.
- Emsellem E, Schinnerer E, Santoro F, Belfiore F, Pessa I, McElroy R, Blanc GA, Congiu E, Groves B, Ho IT, Kreckel K, Razza A, Sanchez-Blazquez P, Egorov O, Faesi C, Klessen RS, Leroy AK, Meidt S, Querejeta M, Rosolowsky E, Scheuermann F, Anand GS, Barnes AT, Be  li   I, Bigiel F, Boquien M, Cao Y, Chevance M, Dale DA, Eibensteiner C, Glover SCO, Grasha K, Henshaw JD, Hughes A, Koch EW, Kruijssen JMD, Lee J, Liu D, Pan HA, Pety J, Saito T, Sandstrom KM, Schrub A, Sun J, Thilker DA, Usero A, Watkins EJ and Williams TG (2022), Mar. The PHANGS-MUSE survey. Probing the chemo-dynamical evolution of disc galaxies. *Astronomy & Astrophysics* 659, A191. doi:10.1051/0004-6361/202141727. 2110.03708.
- Ewen HJ and Purcell EM (1951), Sep. Observation of a Line in the Galactic Radio Spectrum: Radiation from Galactic Hydrogen at 1,420 Mc./sec. *Nature* 168 (4270): 356. doi:10.1038/168356a0.
- Fitzpatrick EL (1999), Jan. Correcting for the Effects of Interstellar Extinction. *PASP* 111 (755): 63–75. doi:10.1086/316293. astro-ph/9809387.
- Fukui Y and Kawamura A (2010), Sep. Molecular Clouds in Nearby Galaxies. *Annual Review of Astronomy & Astrophysics* 48: 547–580. doi:10.1146/annurev-astro-081309-130854.
- Galliano F, Galametz M and Jones AP (2018a), Sep. The Interstellar Dust Properties of Nearby Galaxies. *Annual Review of Astronomy & Astrophysics* 56: 673–713. doi:10.1146/annurev-astro-081817-051900. 1711.07434.
- Galliano F, Galametz M and Jones AP (2018b), Sep. The Interstellar Dust Properties of Nearby Galaxies. *Annual Review of Astronomy & Astrophysics* 56: 673–713. doi:10.1146/annurev-astro-081817-051900. 1711.07434.
- Gao J, Jiang BW, Li A and Xue MY (2013), Oct. The Mid-infrared Extinction Law in the Large Magellanic Cloud. *ApJ* 776 (1), 7. doi:10.1088/0004-637X/776/1/7. 1308.1474.
- Gordon KD, Clayton GC, Misselt KA, Landolt AU and Wolff MJ (2003), Sep. A Quantitative Comparison of the Small Magellanic Cloud, Large Magellanic Cloud, and Milky Way Ultraviolet to Near-Infrared Extinction Curves. *ApJ* 594 (1): 279–293. doi:10.1086/376774. astro-ph/0305257.

- Gordon KD, Clayton GC, Decleir M, Fitzpatrick EL, Massa D, Misselt KA and Tollerud EJ (2023), Jun. One Relation for All Wavelengths: The Far-ultraviolet to Mid-infrared Milky Way Spectroscopic R(V)-dependent Dust Extinction Relationship. *ApJ* 950 (2), 86. doi:10.3847/1538-4357/acb59. 2304.01991.
- Green DA (2014), Jun. A catalogue of 294 Galactic supernova remnants. *Bulletin of the Astronomical Society of India* 42 (2): 47–58. doi:10.48550/arXiv.1409.0637. 1409.0637.
- Hacar A, Clark SE, Heitsch F, Kainulainen J, Panopoulou GV, Seifried D and Smith R (2023), Jul., Initial Conditions for Star Formation: a Physical Description of the Filamentary ISM, Inutsuka S, Aikawa Y, Muto T, Tomida K and Tamura M, (Eds.), *Astronomical Society of the Pacific Conference Series, Astronomical Society of the Pacific Conference Series*, 534, pp. 153.
- Haffner LM, Dettmar RJ, Beckman JE, Wood K, Slavin JD, Giammanco C, Madsen GJ, Zurita A and Reynolds RJ (2009), Jul. The warm ionized medium in spiral galaxies. *Reviews of Modern Physics* 81 (3): 969–997. doi:10.1103/RevModPhys.81.969. 0901.0941.
- Heiles C and Troland TH (2003), Apr. The Millennium Arcicob 21 Centimeter Absorption-Line Survey. II. Properties of the Warm and Cold Neutral Media. *ApJ* 586 (2): 1067–1093. doi:10.1086/367828. astro-ph/0207105.
- Hensley BS and Draine BT (2021), Jan. Observational Constraints on the Physical Properties of Interstellar Dust in the Post-Planck Era. *The Astrophysical Journal* 906 (2), 73. doi:10.3847/1538-4357/abc8f1. 2009.00018.
- Heyer M and Dame TM (2015), Aug. Molecular Clouds in the Milky Way. *Annual Review of Astronomy & Astrophysics* 53: 583–629. doi:10.1146/annurev-astro-082214-122324.
- Hummer DG and Storey PJ (1987), Feb. Recombination-line intensities for hydrogenic ions - I. Case B calculations for H I and He II. *Monthly Notices of the Royal Astronomical Society* 224: 801–820. doi:10.1093/mnras/224.3.801.
- Hunter DA, Elmegreen BG and Baker AL (1998), Jan. The Relationship between Gas, Stars, and Star Formation in Irregular Galaxies: A Test of Simple Models. *The Astrophysical Journal* 493 (2): 595–612. doi:10.1086/305158. astro-ph/9712353.
- Hunter DA, Elmegreen BG and Madden SC (2024), Sep. The Interstellar Medium in Dwarf Irregular Galaxies. *ARA&A* 62 (1): 113–155. doi:10.1146/annurev-astro-052722-104109. 2402.17004.
- Jones AP, Tielens AGGM and Hollenbach DJ (1996), Oct. Grain Shattering in Shocks: The Interstellar Grain Size Distribution. *ApJ* 469: 740. doi:10.1086/177823.
- Kalberla PMW and Kerp J (2009), Sep. The HI Distribution of the Milky Way. *Annual Review of Astronomy & Astrophysics* 47 (1): 27–61. doi:10.1146/annurev-astro-082708-101823.
- Kennicutt Robert C. J (1989), Sep. The Star Formation Law in Galactic Disks. *The Astrophysical Journal* 344: 685. doi:10.1086/167834.
- Kennicutt Robert C. J (1998), May. The Global Schmidt Law in Star-forming Galaxies. *The Astrophysical Journal* 498 (2): 541–552. doi:10.1086/305588. astro-ph/9712213.
- Kennicutt RC and Evans NJ (2012), Sep. Star Formation in the Milky Way and Nearby Galaxies. *Annual Review of Astronomy & Astrophysics* 50: 531–608. doi:10.1146/annurev-astro-081811-125610. 1204.3552.
- Kerr FJ, Hindman JF and Robinson BJ (1954), Jan. Observations of the 21 cm Line from the Magellanic Clouds. *Australian Journal of Physics* 7: 297. doi:10.1071/PH540297.
- Kewley LJ and Ellison SL (2008), Jul. Metallicity Calibrations and the Mass-Metallicity Relation for Star-forming Galaxies. *The Astrophysical Journal* 681 (2): 1183–1204. doi:10.1086/587500. 0801.1849.
- Kewley LJ, Nicholls DC and Sutherland RS (2019), Aug. Understanding Galaxy Evolution Through Emission Lines. *Annual Review of Astronomy & Astrophysics* 57: 511–570. doi:10.1146/annurev-astro-081817-051832. 1910.09730.
- Kim J, Chevance M, Kruijssen JMD, Leroy AK, Schrubba A, Barnes AT, Bigiel F, Blanc GA, Cao Y, Congiu E, Dale DA, Faesi CM, Glover SCO, Grasha K, Groves B, Hughes A, Klessen RS, Kreckel K, McElroy R, Pan HA, Pety J, Querejeta M, Razza A, Rosolowsky E, Saito T, Schinnerer E, Sun J, Tomičić N, Usero A and Williams TG (2022), Oct. Environmental dependence of the molecular cloud lifecycle in 54 main-sequence galaxies. *Monthly Notices of the Royal Astronomical Society* 516 (2): 3006–3028. doi:10.1093/mnras/stac2339. 2206.09857.
- Kormendy J and Kennicutt Robert C. J (2004), Sep. Secular Evolution and the Formation of Pseudobulges in Disk Galaxies. *Annual Review of Astronomy & Astrophysics* 42 (1): 603–683. doi:10.1146/annurev.astro.42.053102.134024. astro-ph/0407343.
- Krumholz MR, McKee CF and Bland-Hawthorn J (2019), Aug. Star Clusters Across Cosmic Time. *Annual Review of Astronomy & Astrophysics* 57: 227–303. doi:10.1146/annurev-astro-091918-104430. 1812.01615.
- Leroy AK, Walter F, Brinks E, Bigiel F, de Blok WJG, Madore B and Thornley MD (2008), Dec. The Star Formation Efficiency in Nearby Galaxies: Measuring Where Gas Forms Stars Effectively. *The Astronomical Journal* 136 (6): 2782–2845. doi:10.1088/0004-6256/136/6/2782. 0810.2556.
- Leroy AK, Walter F, Sandstrom K, Schrubba A, Munoz-Mateos JC, Bigiel F, Bolatto A, Brinks E, de Blok WJG, Meidt S, Rix HW, Rosolowsky E, Schinnerer E, Schuster KF and Usero A (2013), Aug. Molecular Gas and Star Formation in nearby Disk Galaxies. *The Astronomical Journal* 146 (2), 19. doi:10.1088/0004-6256/146/2/19. 1301.2328.
- Leroy AK, Schinnerer E, Hughes A, Rosolowsky E, Pety J, Schrubba A, Usero A, Blanc GA, Chevance M, Emsellem E, Faesi CM, Herrera CN, Liu D, Meidt SE, Querejeta M, Saito T, Sandstrom KM, Sun J, Williams TG, Anand GS, Barnes AT, Behrens EA, Belfiore F, Benincasa SM, Bešlić I, Bigiel F, Bolatto AD, den Brok JS, Cao Y, Chandar R, Chasteney J, Chiang ID, Congiu E, Dale DA, Deger S, Eibensteiner C, Egorov OV, García-Rodríguez A, Glover SCO, Grasha K, Henshaw JD, Ho IT, Képley AA, Kim J, Klessen RS, Kreckel K, Koch EW, Kruijssen JMD, Larson KL, Lee JC, Lopez LA, Machado J, Mayker N, McElroy R, Murphy EJ, Ostriker EC, Pan HA, Pessa I, Puschign J, Razza A, Sánchez-Blázquez P, Santoro F, Sardone A, Scheuermann F, Sliwa K, Sormani MC, Stuber SK, Thilker DA, Turner JA, Utomo D, Watkins EJ and Whitmore B (2021), Dec. PHANGS-ALMA: Arcsecond CO(2-1) Imaging of Nearby Star-forming Galaxies. *The Astrophysical Journal Supplement Series* 257 (2), 43. doi:10.3847/1538-4365/ac17f3. 2104.07739.
- Levine ES, Blitz L and Heiles C (2006), Jun. The Vertical Structure of the Outer Milky Way H I Disk. *ApJ* 643 (2): 881–896. doi:10.1086/503091. astro-ph/0601697.
- Lewis AR, Dolphin AE, Dalcanton JJ, Weisz DR, Williams BF, Bell EF, Seth AC, Simones JE, Skillman ED, Choi Y, Fouesneau M, Guhathakurta P, Johnson LC, Kalirai JS, Leroy AK, Monachesi A, Rix HW and Schrubba A (2015), Jun. The Panchromatic Hubble Andromeda Treasury. XI. The Spatially Resolved Recent Star Formation History of M31. *The Astrophysical Journal* 805 (2), 183. doi:10.1088/0004-637X/805/2/183. 1504.03338.
- Li J, Kreckel K, Sarbadhicary S, Egorov OV, Groves B, Long KS, Congiu E, Belfiore F, Glover SCO, Barnes AT, Bigiel F, Blanc GA, Grasha K, Klessen RS, Leroy A, Lopez LA, Méndez-Delgado JE, Neumann J, Schinnerer E and Williams TG (2024), Oct. Discovery of 2200 new supernova remnants in 19 nearby star-forming galaxies with MUSE spectroscopy. *Astronomy & Astrophysics* 690, A161. doi:10.1051/0004-6361/202450730. 2405.08974.
- Long KS, Blair WP, Winkler PF, Della Bruna L, Adamo A, McLeod AF and Amram P (2022), Apr. Supernova Remnants in M83 as Observed with MUSE. *The Astrophysical Journal* 929 (2), 144. doi:10.3847/1538-4357/ac5aa3. 2202.09929.
- Lopez S, Lopez LA, Nguyen DD, Thompson TA, Mathur S, Bolatto AD, Vulic N and Sardone A (2023), Jan. X-Ray Properties of NGC 253's Starburst-driven Outflow. *The Astrophysical Journal* 942 (2), 108. doi:10.3847/1538-4357/aca65e. 2209.09260.
- Maiolino R and Mannucci F (2019), Feb. De re metallica: the cosmic chemical evolution of galaxies. *Astronomy and Astrophysics Reviews* 27

- (1), 3. doi:10.1007/s00159-018-0112-2. 1811.09642.
- Makarov D, Prugniel P, Terekhova N, Courtois H and Vauglin I (2014), Oct. HyperLEDA. III. The catalogue of extragalactic distances. *Astronomy & Astrophysics* 570, A13. doi:10.1051/0004-6361/201423496. 1408.3476.
- Mangum JG and Shirley YL (2015), Mar. How to Calculate Molecular Column Density. *Publications of the Astronomical Society of the Pacific* 127 (949): 266. doi:10.1086/680323. 1501.01703.
- Mannucci F, Cresci G, Maiolino R, Marconi A and Gnerucci A (2010), Nov. A fundamental relation between mass, star formation rate and metallicity in local and high-redshift galaxies. *MNRAS* 408 (4): 2115–2127. doi:10.1111/j.1365-2966.2010.17291.x. 1005.0006.
- Martig M, Bournaud F, Teyssier R and Dekel A (2009), Dec. Morphological Quenching of Star Formation: Making Early-Type Galaxies Red. *The Astrophysical Journal* 707 (1): 250–267. doi:10.1088/0004-637X/707/1/250. 0905.4669.
- McClure-Griffiths NM, Stanimirović S and Rybarczyk DR (2023), Aug. Atomic Hydrogen in the Milky Way: A Stepping Stone in the Evolution of Galaxies. *Annual Review of Astronomy & Astrophysics* 61: 19–63. doi:10.1146/annurev-astro-052920-104851. 2307.08464.
- Meidt SE, Leroy AK, Querejeta M, Schinnerer E, Sun J, van der Wel A, Emsellem E, Henshaw J, Hughes A, Kruijssen JMD, Rosolowsky E, Schruba A, Barnes A, Bigiel F, Blanc GA, Chevance M, Cao Y, Dale DA, Faesi C, Glover SCO, Grasha K, Groves B, Herrera C, Klessen RS, Kreckel K, Liu D, Pan HA, Pety J, Saito T, Usero A, Watkins E and Williams TG (2021), Jun. The Organization of Cloud-scale Gas Density Structure: High-resolution CO versus 3.6 μm Brightness Contrasts in Nearby Galaxies. *The Astrophysical Journal* 913 (2), 113. doi:10.3847/1538-4357/abf35b. 2103.13247.
- Micelotta ER, Jones AP and Tielens AGGM (2010a), Feb. Polycyclic aromatic hydrocarbon processing in a hot gas. *A&A* 510, A37. doi:10.1051/0004-6361/200911683. 0912.1595.
- Micelotta ER, Jones AP and Tielens AGGM (2010b), Feb. Polycyclic aromatic hydrocarbon processing in interstellar shocks. *A&A* 510, A36. doi:10.1051/0004-6361/200911682. 0910.2461.
- Murphy EJ, Condon JJ, Schinnerer E, Kennicutt RC, Calzetti D, Armus L, Helou G, Turner JL, Aniano G, Beirão P, Bolatto AD, Brandl BR, Croxall KV, Dale DA, Donovan Meyer JL, Draine BT, Engelbracht C, Hunt LK, Hao CN, Koda J, Roussel H, Skibba R and Smith JDT (2011), Aug. Calibrating Extinction-free Star Formation Rate Diagnostics with 33 GHz Free-free Emission in NGC 6946. *The Astrophysical Journal* 737 (2), 67. doi:10.1088/0004-637X/737/2/67. 1105.4877.
- Murray N (2011), Mar. Star Formation Efficiencies and Lifetimes of Giant Molecular Clouds in the Milky Way. *The Astrophysical Journal* 729 (2), 133. doi:10.1088/0004-637X/729/2/133. 1007.3270.
- Obreschkow D and Rawlings S (2009), Apr. Understanding the H₂/HI ratio in galaxies. *MNRAS* 394 (4): 1857–1874. doi:10.1111/j.1365-2966.2009.14497.x. 0901.2526.
- Osterbrock DE and Ferland GJ (2006). *Astrophysics of gaseous nebulae and active galactic nuclei*.
- Ostriker EC and Kim CG (2022), Sep. Pressure-regulated, Feedback-modulated Star Formation in Disk Galaxies. *The Astrophysical Journal* 936 (2), 137. doi:10.3847/1538-4357/ac7de2. 2206.00681.
- Ostriker EC, McKee CF and Leroy AK (2010), Oct. Regulation of Star Formation Rates in Multiphase Galactic Disks: A Thermal/Dynamical Equilibrium Model. *The Astrophysical Journal* 721 (2): 975–994. doi:10.1088/0004-637X/721/2/975. 1008.0410.
- Peeters E, Habart E, Berné O, Sidhu A, Chown R, Van De Putte D, Trahin B, Schroetter I, Canin A, Alarcón F, Scheffer B, Khan B, Pasquini S, Tielens AGGM, Wofire MG, Dartois E, Goicoechea JR, Maragkoudakis A, Onaka T, Pound MW, Vicente S, Abergel A, Bergin EA, Bernard-Salas J, Boersma C, Bron E, Cami J, Cuadrado S, Dicken D, Elyajouri M, Fuente A, Gordon KD, Issa L, Joblin C, Kannaou O, Lacinbala O, Languignoul D, Le Gal R, Meshaka R, Okada Y, Robberto M, Röllig M, Schirmer T, Tabone B, Zannese M, Aleman I, Allamandola L, Auchettl R, Baratta GA, Bejaoui S, Bera PP, Black JH, Boulanger F, Bouwman J, Brandl B, Brechignac P, Brünken S, Buragohain M, Burkhardt A, Candian A, Cazaux S, Cernicharo J, Chabot M, Chakraborty S, Champion J, Colgan SWJ, Cooke IR, Coutens A, Cox NLJ, Demyk K, Meyer JD, Foschino S, García-Lario P, Gerin M, Gottlieb CA, Guillard P, Gusdorf A, Hartigan P, He J, Herbst E, Hornekaer L, Jäger C, Janot-Pacheco E, Kaufman M, Kendrew S, Kirsanova MS, Klaassen P, Kwok S, Labiano Á, Lai TSY, Lee TJ, Lefloch B, Le Petit F, Li A, Linz H, Mackie CJ, Madden SC, Mascetti J, McGuire BA, Merino P, Micelotta ER, Misselt K, Morse JA, Mulas G, Neelamkudan N, Ohsawa R, Paladini R, Palumbo ME, Pathak A, Pendleton YJ, Petrignani A, Pino T, Puga E, Rangwala N, Rapacioli M, Ricca A, Roman-Duval J, Roser J, Roueff E, Rouillé G, Salama F, Sales DA, Sandstrom K, Sarre P, Sciamma-O'Brien E, Sellgren K, Shenoy SS, Teyssier D, Thomas RD, Togi A, Verstraete L, Witt AN, Wooten A, Ysard N, Zettergren H, Zhang Y, Zhang ZE and Zhen J (2024), May. PDRs4All: III. JWST's NIR spectroscopic view of the Orion Bar. *A&A* 685, A74. doi:10.1051/0004-6361/202348244. 2310.08720.
- Peltonen J, Rosolowsky E, Johnson LC, Seth AC, Dalcanton J, Bell EF, Braine J, Koch EW, Lazzarini M, Leroy AK, Skillman ED, Smercina A, Wainer T and Williams BF (2023), Jul. Clusters, clouds, and correlations: relating young clusters to giant molecular clouds in M33 and M31. *Monthly Notices of the Royal Astronomical Society* 522 (4): 6137–6149. doi:10.1093/mnras/stad1430. 2305.03618.
- Pokhrel NR, Simpson CE and Bagetakos I (2020), Aug. A Catalog of Holes and Shells in the Interstellar Medium of the LITTLE THINGS Dwarf Galaxies. *The Astronomical Journal* 160 (2), 66. doi:10.3847/1538-3881/ab9bfa. 2006.01735.
- Portegies Zwart SF, McMillan SLW and Gieles M (2010), Sep. Young Massive Star Clusters. *Annual Review of Astronomy & Astrophysics* 48: 431–493. doi:10.1146/annurev-astro-081309-130834. 1002.1961.
- Querejeta M, Leroy AK, Meidt SE, Schinnerer E, Belfiore F, Emsellem E, Klessen RS, Sun J, Sormani M, Bešić I, Cao Y, Chevance M, Colombo D, Dale DA, García-Burillo S, Glover SCO, Grasha K, Groves B, Koch EW, Neumann L, Pan HA, Pessa I, Pety J, Pinna F, Ramambason L, Razza A, Romanelli A, Rosolowsky E, Ruiz-García M, Sánchez-Blázquez P, Smith R, Stuber S, Ubeda L, Usero A and Williams TG (2024), May. Do spiral arms enhance star formation efficiency? *arXiv e-prints*, arXiv:2405.05364doi:10.48550/arXiv.2405.05364. 2405.05364.
- Rachford BL, Snow TP, Destree JD, Ross TL, Ferlet R, Friedman SD, Gry C, Jenkins EB, Morton DC, Savage BD, Shull JM, Sonnentrucker P, Tumlinson J, Vidal-Madjar A, Welty DE and York DG (2009), Jan. Molecular Hydrogen in the Far Ultraviolet Spectroscopic Explorer Translucent Lines of Sight: The Full Sample. *ApJS* 180 (1): 125–137. doi:10.1088/0067-0049/180/1/125. 0809.3831.
- Rémy-Ruyer A, Madden SC, Galliano F, Galametz M, Takeuchi TT, Asano RS, Zhukovska S, Lebouteiller V, Cormier D, Jones A, Bocchio M, Baes M, Bendo GJ, Boquien M, Boselli A, DeLooze I, Doublier-Pritchard V, Hughes T, Karczewski OŁ and Spinoglio L (2014), Mar. Gas-to-dust mass ratios in local galaxies over a 2 dex metallicity range. *A&A* 563, A31. doi:10.1051/0004-6361/201322803. 1312.3442.
- Rieke GH and Lebofsky MJ (1985), Jan. The interstellar extinction law from 1 to 13 microns. *ApJ* 288: 618–621. doi:10.1086/162827.
- Rosenthal D, Bertoldi F and Drapatz S (2000), Apr. ISO-SWS observations of OMC-1: H₂ and fine structure lines. *A&A* 356: 705–723. doi:10.48550/arXiv.astro-ph/0002456. astro-ph/0002456.
- Ryden BS and Pogge RW (2021). *Interstellar and intergalactic medium*. doi:10.1017/9781108781596.
- Saintonge A and Catinella B (2022), Aug. The Cold Interstellar Medium of Galaxies in the Local Universe. *Annual Review of Astronomy & Astrophysics* 60: 319–361. doi:10.1146/annurev-astro-021022-043545. 2202.00690.
- Saintonge A, Catinella B, Tacconi LJ, Kauffmann G, Genzel R, Cortese L, Davé R, Fletcher TJ, Graciá-Carpio J, Kramer C, Heckman TM, Janowiecki S, Lutz K, Rosario D, Schiminovich D, Schuster K, Wang J, Wuyts S, Borthakur S, Lamperti I and Roberts-Borsani GW (2017), Dec. xCOLD GASS: The Complete IRAM 30 m Legacy Survey of Molecular Gas for Galaxy Evolution Studies. *The Astrophysical Journal Supplement Series* 233 (2), 22. doi:10.3847/1538-4365/aa97e0. 1710.02157.

- Sánchez SF (2020), Aug. Spatially Resolved Spectroscopic Properties of Low-Redshift Star-Forming Galaxies. *Annual Review of Astronomy & Astrophysics* 58: 99–155. doi:10.1146/annurev-astro-012120-013326. 1911.06925.
- Sánchez SF, Kennicutt RC, Gil de Paz A, van de Ven G, Vílchez JM, Wisotzki L, Walcher CJ, Mast D, Aguerri JAL, Albiol-Pérez S, Alonso-Herrero A, Alves J, Bakos J, Bartáková T, Bland-Hawthorn J, Boselli A, Bomans DJ, Castillo-Morales A, Cortijo-Ferrero C, de Lorenzo-Cáceres A, Del Olmo A, Dettmar RJ, Díaz A, Ellis S, Falcón-Barroso J, Flores H, Gallazzi A, García-Lorenzo B, González Delgado R, Gruel N, Haines T, Hao C, Husemann B, Iglésias-Páramo J, Jahnke K, Johnson B, Jungwiert B, Kalinova V, Kehrig C, Kupko D, López-Sánchez AR, Lyubenova M, Marino RA, Mármol-Queraltó E, Márquez I, Masegosa J, Meidt S, Mendez-Abreu J, Monreal-Ibero A, Montijo C, Mourão AM, Palacios-Navarro G, Papaderos P, Pasquali A, Peletier R, Pérez E, Pérez I, Quirrenbach A, Relaño M, Rosales-Ortega FF, Roth MM, Ruiz-Lara T, Sánchez-Blázquez P, Sengupta C, Singh R, Stanishev V, Trager SC, Vazdekis A, Viironen K, Wild V, Zibetti S and Ziegler B (2012), Feb. CALIFA, the Calar Alto Legacy Integral Field Area survey. I. Survey presentation. *Astronomy & Astrophysics* 538, A8. doi:10.1051/0004-6361/201117353. 1111.0962.
- Sancisi R, Fraternali F, Oosterloo T and van der Hulst T (2008), Jun. Cold gas accretion in galaxies. *Astronomy and Astrophysics Reviews* 15 (3): 189–223. doi:10.1007/s00159-008-0010-0. 0803.0109.
- Sanders DB and Mirabel IF (1996), Jan. Luminous Infrared Galaxies. *ARA&A* 34: 749. doi:10.1146/annurev.astro.34.1.749.
- Schinnerer E and Leroy AK (2024), Mar. Molecular Gas and the Star Formation Process on Cloud Scales in Nearby Galaxies. *arXiv e-prints*, arXiv:2403.19843doi:10.48550/arXiv.2403.19843. 2403.19843.
- Schruba A, Leroy AK, Walter F, Sandstrom K and Rosolowsky E (2010), Oct. The Scale Dependence of the Molecular Gas Depletion Time in M33. *The Astrophysical Journal* 722 (2): 1699–1706. doi:10.1088/0004-637X/722/2/1699. 1009.1651.
- Schruba A, Leroy AK, Walter F, Bigiel F, Brinks E, de Blok WJG, Dumas G, Kramer C, Rosolowsky E, Sandstrom K, Schuster K, Usero A, Weiss A and Wiesemeyer H (2011), Aug. A Molecular Star Formation Law in the Atomic-gas-dominated Regime in Nearby Galaxies. *The Astronomical Journal* 142 (2), 37. doi:10.1088/0004-6256/142/2/37. 1105.4605.
- Sellgren K (1984), Feb. The near-infrared continuum emission of visual reflection nebulae. *ApJ* 277: 623–633. doi:10.1086/161733.
- Shirley YL (2015), Mar. The Critical Density and the Effective Excitation Density of Commonly Observed Molecular Dense Gas Tracers. *Publications of the Astronomical Society of the Pacific* 127 (949): 299. doi:10.1086/680342. 1501.01629.
- Silk J (1997), May. Feedback, Disk Self-Regulation, and Galaxy Formation. *The Astrophysical Journal* 481 (2): 703–709. doi:10.1086/304073. astro-ph/9612117.
- Solomon PM and Vanden Bout PA (2005), Sep. Molecular Gas at High Redshift. *ARA&A* 43 (1): 677–725. doi:10.1146/annurev.astro.43.051804.102221. astro-ph/0508481.
- Spitzer Lyman J (1968), Dynamics of Interstellar Matter and the Formation of Stars, Middlehurst BM and Aller LH, (Eds.), *Nebulae and Interstellar Matter*, pp. 1.
- Stuber SK, Schinnerer E, Williams TG, Querejeta M, Meidt S, Emsellem É, Barnes A, Klessen RS, Leroy AK, Neumann J, Sormani MC, Bigiel F, Chevance M, Dale D, Faesi C, Glover SCO, Grasha K, Diederik Kruijssen JM, Liu D, Pan Ha, Pety J, Pinna F, Saito T, Usero A and Watkins EJ (2023), Aug. The gas morphology of nearby star-forming galaxies. *Astronomy & Astrophysics* 676, A113. doi:10.1051/0004-6361/202346318. 2305.17172.
- Sun J, Leroy AK, Ostriker EC, Meidt S, Rosolowsky E, Schinnerer E, Wilson CD, Utomo D, Belfiore F, Blanc GA, Emsellem E, Faesi C, Groves B, Hughes A, Koch EW, Kreckel K, Liu D, Pan HA, Pety J, Querejeta M, Razza A, Saito T, Sardone A, Usero A, Williams TG, Bigiel F, Bolatto AD, Chevance M, Dale DA, Gensior J, Glover SCO, Grasha K, Henshaw JD, Jiménez-Donaire MJ, Klessen RS, Kruijssen JMD, Murphy EJ, Neumann L, Teng YH and Thilker DA (2023), Mar. Star Formation Laws and Efficiencies across 80 Nearby Galaxies. *The Astrophysical Journal Letters* 945 (2), L19. doi:10.3847/2041-8213/acbd9c. 2302.12267.
- Tacconi LJ, Genzel R and Sternberg A (2020), Aug. The Evolution of the Star-Forming Interstellar Medium Across Cosmic Time. *Annual Review of Astronomy & Astrophysics* 58: 157–203. doi:10.1146/annurev-astro-082812-141034. 2003.06245.
- Thompson TA and Heckman TM (2024), Sep. Theory and Observation of Winds from Star-Forming Galaxies. *Annual Review of Astronomy & Astrophysics* 62 (1): 529–591. doi:10.1146/annurev-astro-041224-011924. 2406.08561.
- Tielens AGGM (2005). The Physics and Chemistry of the Interstellar Medium.
- Tielens AGGM (2008), Sep. Interstellar polycyclic aromatic hydrocarbon molecules. *Annual Review of Astronomy & Astrophysics* 46: 289–337. doi:10.1146/annurev.astro.46.060407.145211.
- Tremonti CA, Heckman TM, Kauffmann G, Brinchmann J, Charlot S, White SDM, Seibert M, Peng EW, Schlegel DJ, Uomoto A, Fukugita M and Brinkmann J (2004), Oct. The Origin of the Mass-Metallicity Relation: Insights from 53,000 Star-forming Galaxies in the Sloan Digital Sky Survey. *ApJ* 613 (2): 898–913. doi:10.1086/423264. astro-ph/0405537.
- Tumlinson J, Peebles MS and Werk JK (2017), Aug. The Circumgalactic Medium. *ARA&A* 55 (1): 389–432. doi:10.1146/annurev-astro-091916-055240. 1709.09180.
- van de Hulst HC (1945), Jan. Radiogolven uit het wereldruim: II. Herkomst der radiogolvenRadiogolven uit het wereldruim: II. Herkomst der radiogolvenRadio waves from space. *Nederlandsch Tijdschrift voor Natuurkunde* 11: 210–221.
- Veilleux S and Osterbrock DE (1987), Feb. Spectral Classification of Emission-Line Galaxies. *The Astrophysical Journal Supplement Series* 63: 295. doi:10.1086/191166.
- Veilleux S, Maiolino R, Bolatto AD and Aalto S (2020), Apr. Cool outflows in galaxies and their implications. *Astronomy and Astrophysics Reviews* 28 (1), 2. doi:10.1007/s00159-019-0121-9. 2002.07765.
- Wang J, Koribalski BS, Serra P, van der Hulst T, Roychowdhury S, Kamphuis P and Chengalur JN (2016), Aug. New lessons from the H I size-mass relation of galaxies. *Monthly Notices of the Royal Astronomical Society* 460 (2): 2143–2151. doi:10.1093/mnras/stw1099. 1605.01489.
- Wang QD, Zeng Y, Bogdán A and Ji L (2021), Dec. Deep Chandra observations of diffuse hot plasma in M83. *Monthly Notices of the Royal Astronomical Society* 508 (4): 6155–6175. doi:10.1093/mnras/stab2997. 2110.06995.
- Wisnioski E, Glazebrook K, Blake C, Poole GB, Green AW, Wyder T and Martin C (2012), Jun. Scaling relations of star-forming regions: from kpc-sized clumps to H II regions. *Monthly Notices of the Royal Astronomical Society* 422 (4): 3339–3355. doi:10.1111/j.1365-2966.2012.20850.x. 1203.0309.
- Witt AN and Lai TSY (2020), Mar. Extended red emission: observational constraints for models. *Ap&SS* 365 (3), 58. doi:10.1007/s10509-020-03766-w. 2003.06453.
- Wolfire MG, Vallini L and Chevance M (2022), Aug. Photodissociation and X-Ray-Dominated Regions. *ARA&A* 60: 247–318. doi:10.1146/annurev-astro-052920-010254. 2202.05867.
- Wong T and Blitz L (2002), Apr. The Relationship between Gas Content and Star Formation in Molecule-rich Spiral Galaxies. *The Astrophysical Journal* 569 (1): 157–183. doi:10.1086/339287. astro-ph/0112204.
- Wright EL, Eisenhardt PRM, Mainzer AK, Ressler ME, Cutri RM, Jarrett T, Kirkpatrick JD, Padgett D, McMillan RS, Skrutskie M, Stanford SA, Cohen M, Walker RG, Mather JC, Leisawitz D, Gautier Thomas N. I, McLean I, Benford D, Lonsdale CJ, Blain A, Mendez B, Irace WR, Duval V, Liu F, Royer D, Heinrichsen I, Howard J, Shannon M, Kendall M, Walsh AL, Larsen M, Cardon JG, Schick S, Schwalm M, Abid M, Fabinsky

- B, Naes L and Tsai CW (2010), Dec. The Wide-field Infrared Survey Explorer (WISE): Mission Description and Initial On-orbit Performance. The Astronomical Journal 140 (6): 1868–1881. doi:10.1088/0004-6256/140/6/1868. 1008.0031.
- Young JS and Knezek PM (1989), Dec. The Ratio of Molecular to Atomic Gas in Spiral Galaxies as a Function of Morphological Type. ApJL 347: L55. doi:10.1086/185606.
- Young JS and Scoville NZ (1991), Jan. Molecular gas in galaxies. Annual Review of Astronomy & Astrophysics 29: 581–625. doi:10.1146/annurev.aa.29.090191.003053.
- Young JS, Xie S, Tacconi L, Knezek P, Viscuso P, Tacconi-Garman L, Scoville N, Schneider S, Schloerb FP, Lord S, Lesser A, Kenney J, Huang YL, Devereux N, Claussen M, Case J, Carpenter J, Berry M and Allen L (1995), May. The FCRAO Extragalactic CO Survey. I. The Data. The Astrophysical Journal Supplement Series 98: 219. doi:10.1086/192159.
- Young JS, Allen L, Kenney JDP, Lesser A and Rownd B (1996), Nov. The Global Rate and Efficiency of Star Formation in Spiral Galaxies as a Function of Morphology and Environment. The Astronomical Journal 112: 1903. doi:10.1086/118152.